Chapter 3

Hydrodynamics

David M. Paterson

Over the last decades, fluid dynamics has undergone a revolution in the understanding of the importance of flow to the ecology of aquatic ecosystems. This advance has been driven in two ways: firstly as a by-product of improved system analysis that allows the determination of flow patterns at ever decreasing scales of space and time; Secondly, many new methods have been specifically developed to examine questions in ecology that are related to flow dynamics and the behavior of organism in response to flow. Early work was fairly predictable, employing standard fluid dynamics approaches to test biological theory under laboratory conditions (e.g., "flume and flora" experiments), then a period began in which many laboratories produced devices to measure the stability of sediment under field conditions, including fully submerged marine systems. Examples range from linear flumes, carousel or circular chamber systems, to suction or jet devices. These systems all produce useful data but rarely on a comparative scale across ecosystems. The size of the imprint, the nature of the flow created and the method of determining the point of incipient erosion all vary. These are ongoing problems that cannot easily be addressed but of further interest is the imbalance in the applications of these techniques across the fields of research that have developed and applied these technologies. Far more information in terms of relative sediment stability and biogenic interactions is available in the literature concerning brackish (estuarine) and marine environments than fresh water systems. This is perhaps surprising since the overarching characteristic of fluvial systems is the continual longitudinal displacement of the medium … the river flow. The sediment of river system is continually in motion and undergo catastrophic redistribution during extreme episodic events. These systems are therefore vulnerable to hydrodynamic forcing and the complex control of sediment dynamics is worthy of further consideration. The understanding of the stability of natural fluvial sediments and their behavior on erosion is a fundamental part of the suite of research. The sections in the following chapter help to redress this balance. In the first paper, Spears et al. make an explicit the comparison of sediment stability across different systems, providing an unusual direct comparison between fresh water and brackish habitats. For this work, a single stability device was applied across the varied system which allows for confidence in their comparative approach. In contrast, Gerbersdorf et al. consider the "strength with depth" of natural sediment systems. The novelty of their approach is in determining depth profiles of variables, such as bed shear stress, but linked to the biological and physicochemical properties of the sediment. They argue that this is important in predicting the nature of the bed failure and consequent transport of material, which may also include contaminants from the river system. The behavior of material after erosion is also of critical importance and Mueller

et al. continue their well-known ability to produce novel engineering methods and approaches by introducing the *B*enthic *W*ater *C*olumn *S*imulator (BWCS). This engineering device allows experimental investigation of particles and floc throughout the simulated cycle of erosion, transportation, deposition and consolidation of fine sediments. A further engineering approach is presented by Kuehn and Jirka with the objective of creating a system in which turbulence can be controlled and varied over the depth of a water column, essentially separating advection from turbulent intensity regime. This is an innovative approach that will allow the introduction of biological variables into the design system of great engineering precision. Each of these contributions is innovative in its own way and outlines the great potential in combining engineering approaches to answer current questions in the field of fluvial sediment transport.

Bryan M. Spears · Jenna Funnell · James Saunders · David M. Paterson

3.1 On the Boundaries: Sediment Stability Measurements across Aquatic Ecosystems

3.1.1 Introduction

Few studies in the literature compare the sediment stability of depositional habits across marine, freshwater and brackish ecosystems. This is partly because there is conceptual difficulty in comparing different erosional devices but also because scientist often focus on specific habitats. In addition, many field devices generate shear stresses over the 0–1 N m^{-2} range, with few capable of generating erosive forces beyond this level (Tolhurst et al. 2000). However, habitats such as intertidal deposits and salt marshes are often quite resistant to hydrodynamic forcing and are considered to provide an "ecosystem service" of coastal protection. Most existing measurements have been made within a "measurement comfort zone" (Fig. 3.1), usually where a bed shear stress between approximately 0.1 and 1 N m^{-2} surpasses the critical threshold. However, the study of a wider range of habitats is fundamental to the understanding of ecosystem dynamics in aquatic environments.

Resistance to sediment disturbance can be enhanced via physicochemical (particle-particle attraction/resistance; Lerman 1979; Lick and Huang 1993), bio-physical (e.g., increased structural integrity within root beds; Kenworthy et al. 1982; Benoy and Kalff 1999) and bio-chemical processes (the production of extracellular polymeric substances: EPS) (Paterson 1994; Yallop et al. 2000; Deco 2000). While the majority of field based sediment stability studies have been conducted within estuarine mudflat ecosystems, the relevance of these findings across different sediment ecosystems remains largely unknown. Variation should be expected since significant variations in ecosystem processes, known to affect sediment stability, occur within, and between, different ecosystems (e.g., lakes, rivers, and estuaries). These include exposure/submersion cycles, the deposition/removal of fine particulate matter (FPM), the community structure of benthic fauna and flora, and the shear stress exerted across the sediment surface (O'Sullivan and Reynolds 2004; Nedwell and Raffaelli 1999).

In estuarine systems, the presence of EPS, secreted mainly by benthic diatoms (Goto et al. 1999; Yallop et al. 2000), has been shown to enhance sediment stability (see Paterson

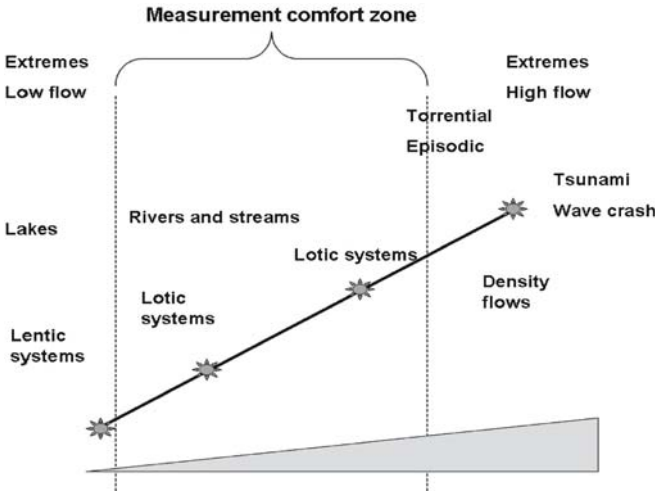

Fig. 3.1.
Schematic diagram of the measurement comfort zone for many erosion devices

1997; Tolhurst 1999; Decho 2000). Recent studies have also highlighted the role of vascular plant root-systems in enhancing sediment stability and accumulation by increasing the structural integrity and, therefore, the bed shear strength of colonized riverine and estuarine sediments (Grady 1981). Similar ecosystem engineering may occur in shallow freshwater lakes in which light regimes favor the colonization of macrophytes and microphytobenthos. However, a number of differences occur between ecosystems. For example, tidal cycles drive diurnal fluctuations in estuarine sediment exposure/submersion and compaction. In contrast, lacustrine sediments are continually submerged, with fewer disturbances and a higher depositional flux of fine particulate matter. Another key difference between freshwater and estuarine systems is the strength of the electrostatic attractions (cohesion) between sediment particles as influenced by salinity (Packman and Jerolmack 2004).

A relatively simple comparative assessment of sediment stability across estuarine and freshwater habitats, using the same measurement system, was undertaken. Additionally, spatial variation within each ecosystem was assessed (lake depth, intertidal position). The specific objectives of the study were to *(1)* assess the spatial variation (i.e. inter- and intra-site) of sediment stability and related sediment characteristics; *(2)* identify the key variables regulating stability in each site; and *(3)* identify trends in stability regulation across ecosystem types.

3.1.2 Methods

Study Sites

Loch Leven is a shallow eutrophic loch situated in the southeast of Scotland (56°10' N, 3°30' W), with a mean depth of 3.9 m, covers an area of 13.7 km^2 and is generally dominated by *Potamogeton* sp. Two sample sites were chosen at 2.1 m (shallow Loch Leven site) and 4.3 m (deep Loch Leven site) depth (Fig. 3.2) to represent macrophyte and microphytobenthos dominated sediment, respectively.

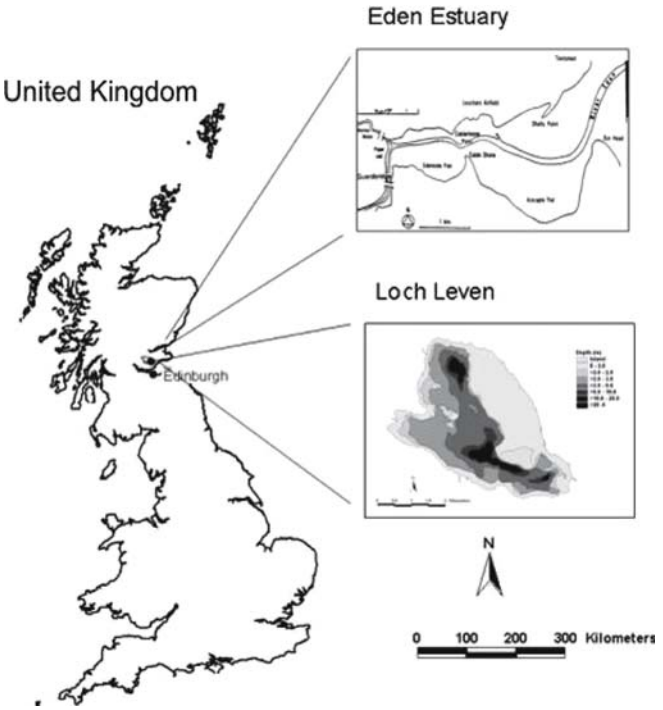

Fig. 3.2.
Map showing sample sites within Loch Leven and the Eden Estuary

The Eden Estuary is situated in southeast Scotland (56°22' N, 2°50' W) and is composed of both mudflat (8 km^2 surface area) and saltmarsh (0.11 km^2). The mudflat is generally dominated by microphytobenthos (mainly diatoms) and the saltmarsh mainly by *Puccinellia maritima*. Three sample sites were chosen on the southern shore near the mouth of the estuary to represent low shore and mid shore mudflat, and saltmarsh sediment areas (Fig. 3.2). Sediment is predominantly sandy mud.

Sample Collection

20 cores were collected from each site (i.e. 100 cores in total). At each site, 10 cores were used for stability analysis and 10 cores for the quantification of other sediment characteristics. In the latter, the upper 2 mm of sediment was cryogenically preserved using the contact coring technique (HIMOM 2005). Cores (8 cm internal diameter and 5 cm deep) were collected manually (7–15 February, 2006) from within a 2 m^2 area of exposed sediment at both mudflat sites and the saltmarsh site. To maintain the natural structure of the sediment, macrophytes present in the saltmarsh cores were not removed. Freshwater sediment cores (6.7 cm internal diameter) were collected (21 March 2006 by boat) at each site, within a 10 m^2 area of submerged sediment using a Jenkin surface-sediment sampler. The cores consisted of 20 cm sediment overlain by 30 cm water. The overlying water was either left (for the analysis of sediment stability) or carefully siphoned off to leave an exposed sediment surface as required for contact coring.

Sediment Stability

Sediment stability was measured using a Mark IV Cohesive Strength Meter (CSM) (Paterson et al. 1989). The CSM operates by firing a sequence of water jets with incremental increases in pressure onto the sediment surface inside a small (2 cm diameter) erosion chamber filled with filtered seawater. Eroded sediment is detected by an infrared transmission across the inside of the erosion chamber. The critical erosion threshold is deemed to have passed when suspended sediment levels result in a 10% drop in the original transmission value encountered at the beginning of the test (Tolhurst et al. 2000). The test program "Fine 1" was selected due to its high resolution at low critical erosion thresholds which were expected after initial trials upon the sediments. The CSM was calibrated and results expressed as the stagnation pressure upon the sediment surface expressed as N m^{-2}.

Cores ($n = 10$) from the saltmarsh and mudflat sites were analyzed in the laboratory. The erosion chamber was set flush with the exposed sediment surface and manually filled with filtered saline water by syringe. Stability in freshwater cores was analyzed immediately after collection and with the overlying water column intact. Filtered saline water was used as the erosive medium in saltmarsh and mudflat cores.

Other Sediment Characteristics

At each site, 10 contact cores were collected for the analysis of wet bulk density, water content, and organic content (HIMOM protocols 2005). Bound and colloidal carbohydrates were separated following the addition of 5 ml distilled water to 50 mg freeze dried sediment and subsequent centrifugation (1 500 rpm for 15 minutes). The resultant pellet was analyzed for bound (attached), and the supernatant colloidal, carbohydrates (Underwood et al. 1995). Both colloidal and bound carbohydrate concentrations were determined using Dubois assays as described within HIMOM protocols (2005) and are expressed against a glucose standard curve as glucose equivalents (μg g^{-1} dry weight glucose equivalents). Chlorophyll *a* was extracted from freeze dried sediment in 90% acetone. The extraction was conducted at –4 °C in an ultrasound bath for 90 min. Following this, samples were stored in the dark at –80 °C for 24 hours before being vortexed and stored for a further 24 h in the same conditions. Samples were centrifuged (2000 rpm) for 3 min prior to spectrophotometric pigment analysis according to HIMOM (2005).

Statistical Analysis

Statistical variation was assessed using one-way analysis of variance (ANOVA) followed by Fisher's least significant difference post-hoc analysis (critical value = 2.014, $\alpha = 0.05$), on observation of a significant ANOVA result. An analysis of the relationships between variables within each site (intra-site relationships) was conducted using correlation analysis ($n = 10$). An analysis of the relationships between variables across the five sites (inter-site relationships) was also conducted using correlation analysis ($n = 5$). All error bars shown represent the standard error of the mean ($n = 10$) taken from each variable.

3.1.3 Results and Discussion

Variation in Sediment Stability Properties between Ecosystem Types

Significant intra-site variation (Table 3.1 and Fig. 3.3; ANOVA analyses; $p < 0.05$) was observed in sediment stability, colloidal carbohydrate concentration, bound carbohydrate concentration, chlorophyll *a* concentration, organic matter content, water content, and bulk density. Sediment stability was lowest in the freshwater sites, intermediate in the mudflat sites and highest in the saltmarsh site. Stability was observed to increase with depth in the freshwater sites and with increasing distance up the shore in the estuary. The saltmarsh site was more stable than the intertidal low shore site, the shallow and deep freshwater sites. Sediment stability was significantly higher for the mid shore intertidal site than it was in the shallow freshwater site (Fig. 3.3a). Colloidal carbohydrate and bound carbohydrate concentrations were significantly higher in the deep freshwater site than at all other sites (Fig. 3.3b). The bound carbohydrate concentration in the shallow freshwater site was higher than for mid and low shore mudflat sites but similar to the values observed in the saltmarsh site (Fig. 3.3c). Chlorophyll *a* concentration was significantly higher in the deep freshwater site than any other site (Fig. 3.3d). The salt marsh and the shallow freshwater site had similar chlorophyll *a* concentrations, both being higher than the mudflat sites. Sediment organic content was similar for salt marsh and the deep freshwater sites which were both significantly higher than all other sites (Fig. 3.3e). The water content of the mudflat sites were both low and did not differ from each other. Intermediate water content was observed in the saltmarsh site followed by the shallow freshwater site with the highest water content observed in the deep freshwater site (Fig. 3.3f). The bulk density of the intertidal sites were greatest, followed by the salt marsh site and then the freshwater sites. Bulk density in the mid shore site was significantly greater than all other sites with the exception of the low shore tidal site (Fig. 3.3g).

Intra-Site Relationships between Sediment Stability Properties

A positive correlation between sediment stability and colloidal carbohydrate concentration was found for the deep freshwater site (Table 3.2). Negative correlations were observed between sediment stability and chlorophyll *a*, and sediment stability and organic content in the mid shore tidal site and between sediment stability and bulk density in the salt marsh site. Sediment stability was not significantly correlated with any of the measured variables in the shallow freshwater site or the low shore site.

Inter-Site Relationships between Sediment Stability Properties

No significant relationships were observed between sediment stability and any of the other measured variables across the sites. Colloidal carbohydrate, bound carbohydrate and chlorophyll *a* concentrations were significantly positively inter-correlated. The measured sediment characteristics varied significantly both across and within the five sites. The majority of these differences can be accounted for by considering the key ecosystem processes acting within each. Within the estuarine environment,

Table 3.1.
Summary of results taken from Fishers post hoc analysis. Direct comparisons of primary variables versus all other variables included where '+' represents instances where primary variables are higher than other variables and '–' represents instances where the primary variable is less than other variables

Primary variable	2.1 m	4.3 m	Low	Mid
Sediment stability				
2.1 m				–
4.3 m				–
Low				
Mid			+	
Salt	+	+	+	+
Colloidal carbohydrates				
2.1 m		+		
4.3 m				
Low		+		
Mid		+		
Salt		+		
Bound carbohydrates				
2.1 m			+	+
4.3 m	+		+	+
Low				
Mid				
Salt	–	–	+	+
Chlorophyll *a*				
2.1 m			+	+
4.3 m	+		+	+
Low				
Mid				
Salt		–	+	+
Organic matter content				
2.1 m				
4.3 m	+		+	+
Low				
Mid				
Salt	+		+	+
Water content				
2.1 m			+	+
4.3 m	+		+	+
Low				
Mid			+	
Salt	–	–	+	+
Bulk density				
2.1 m			–	–
4.3 m			–	–
Low				
Mid				
Salt	+	+	–	–

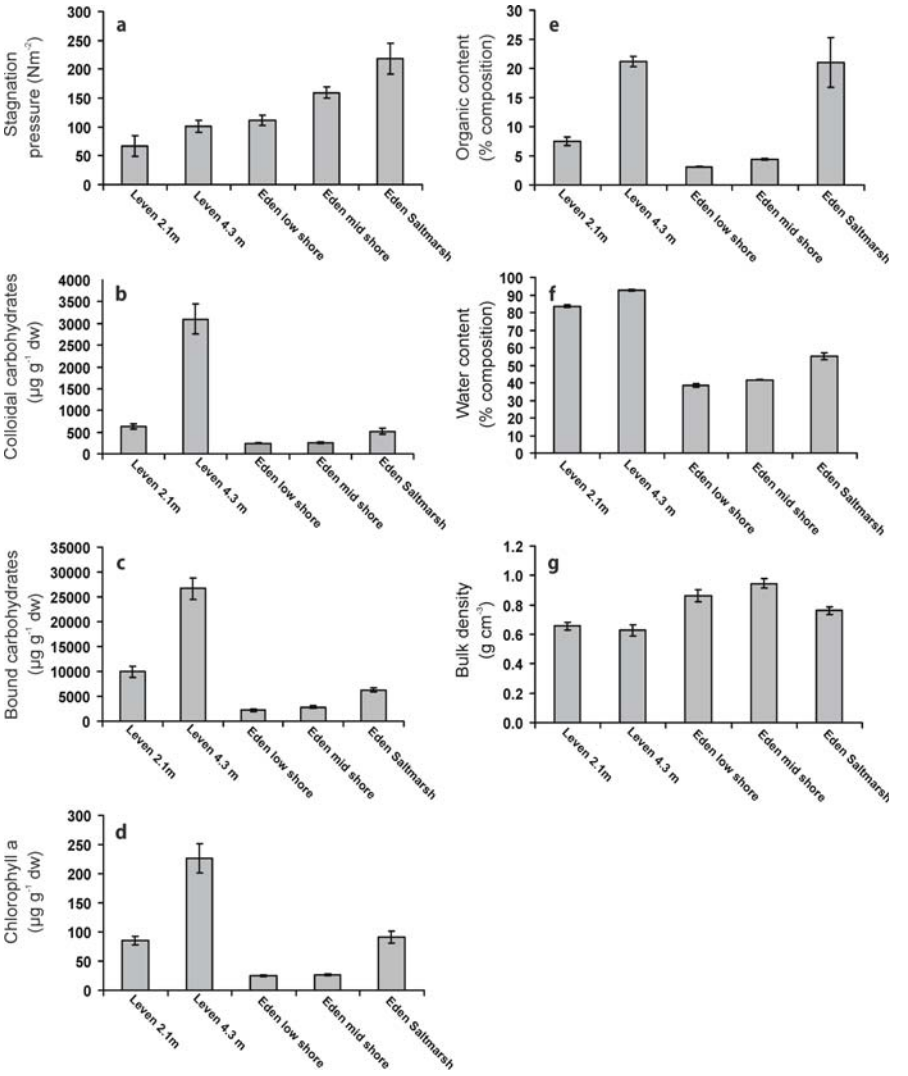

Fig. 3.3. Average cross site trends in **a** stagnation pressure that corresponds to the critical erosion threshold, **b** colloidal carbohydrate concentration, **c** bound carbohydrate concentration, **d** chlorophyll *a* concentration, **e** organic content, **f** water content, and **g** wet bulk density. Error bars represent the standard error of the mean ($n = 10$)

bulk density was lowest in the saltmarsh site and similar in both low and mid shore sediment. This is probably the result of a number of factors including bioturbation, the effect of vegetative cover on the salt marsh and the consequent retention of fine sediments. In comparison, the bulk density values of both freshwater sites were significantly lower than all the estuarine sites. This is due to the depositional environment in productive freshwater lakes where high fluxes of FPM and flocs are combined

Table 3.2. Summary of correlation analysis ($n = 10$; $p < 0.05$) for each site. Only significant correlations reported. *Coll. carb:* Colloidal carbohydrates; *Bound carb.:* bound carbohydrates; *Chl. a:* chlorophyll a; *Org.:* Organic content; *Bulk den.:* bulk density.

Relations	Variable *X*	Variable *Y*	*P*-value	R^2
Loch Leven 2.1 m	Coll. carb.	Chl. *a*	0.043	0.65
	Coll. carb.	Bulk den.	0.021	–0.71
	Bulk den.	Water	0.025	–0.70
	Chl. *a*	Org.	0.043	0.64
Loch Leven 4.3 m	Stability	Coll. carb.	0.032	0.675
	Coll. carb.	Water	0.002	0.85
	Bound carb.	Chl. *a*	0.009	–0.77
	Chl. *a*	Water	0.015	0.74
Eden low shore	Chl. *a*	Org.	0.007	0.79
	Water	Chl. *a*	0.014	0.74
	Water	Org.	0.004	0.81
Eden mid shore	Stability	Chl. *a*	0.044	–0.64
	Stability	Org.	0.016	–0.73
	Coll. carb.	Bound carb.	0.016	0.73
	Chl. *a*	Org.	0.011	0.76
	Chl. *a*	Water	0.034	0.67
	Org.	Water	0.008	0.78
	Bulk den.	Water	0.013	–0.75
Eden saltmarsh	Stability	Bulk den.	0.033	–0.67
	Coll. carb.	Chl. *a*	0.028	0.69
	Coll. carb.	Org.	0.013	0.75
	Coll. carb.	Water	0.025	0.70
	Chl. *a*	Org.	0.000	0.90

with low sediment flushing rates (Hilton et al. 1986; Weyenmeyer at al. 1995). These processes result in the accumulation of fine, unconsolidated organic matter (Nedwell et al. 1999).

Water content was expected to decrease up the shore line as a result of increased exposure and evaporation. However, the opposite trend was observed, most likely resulting from biologically-mediated ecosystem engineering where biofilms and rooted plant beds can trap moisture and prevent desiccation (Paterson and Black 1999; Yallop et al. 2000).

Chlorophyll a, Organic Matter, and Carbohydrate Concentrations

Similar trends in chlorophyll *a* concentration, organic matter content, and bound and colloidal carbohydrate concentrations were observed across the sites. The correlations between chlorophyll *a* concentration and bound and colloidal carbohydrate concentrations within freshwater and saltmarsh sediments suggest that the main source of carbohydrates in these systems are derived from autotrophic processes (Table 3.2). The absence of a significant correlation between chlorophyll *a* and carbohydrate concentrations in the mudflat sites agrees with the observations of Perkins et al. (2003) in which carbohydrate concentration was shown to be more sensitive to a simulated tidal cycle than chlorophyll *a* concentration as a result of the greater solubility of carbohydrates in water. Thus, an uncoupling of the two variables can be expected in sediment ecosystems exposed to severe tidal processes. Both bound and colloidal carbohydrate concentrations were higher in freshwater than they were in estuarine sediments. Coupled with the chlorophyll *a* concentrations, this suggests that the highest autotrophic production of carbohydrates occurred in freshwater sediment which may be due to the relatively high autotrophic (i.e. combination of phytoplankton, microphytobenthos, epiphytes etc.) production in these high nutrient systems.

The higher chlorophyll *a* values in the freshwater sites compared to the mudflat sites are likely due to a higher accumulation of phytoplanktonic detritus. This process is especially important in eutrophic lakes where movement of phytoplankton between the sediment and the water column is regulated by environmental variables and can account for major portions of total phosphorus and nitrogen partitioning (Head et al. 1999). The high organic content and chlorophyll *a* concentrations observed in the saltmarsh, in comparison to the mudflat sites, is likely due to an increase

Table 3.3. Correlation analysis of sediment characteristics across five sites (Loch Leven 2.2 m, Loch Leven 4.3 m, Eden low shore, Eden mid shore, and Eden saltmarsh). *Coll. carb:* Colloidal carbohydrates; *Bound carb.:* bound carbohydrates; *Chl. a:* chlorophyll *a*; *Org.:* Organic content; *Bulk den.:* bulk density. Significant correlations in bold with *p* values in parenthesis

	Stability	Coll. carb.	Bound carb.	Chl. *a*	Org.	Water
Coll. carb.	–0.309 (0.613)					
Bound. carb.	–0.371 (0.538)	**0.984 (0.002)**				
Chl. *a*	–0.223 (0.718)	**0.966 (0.008)**	**0.983 (0.003)**			
Org.	0.360 (0.552)	0.662 (0.223)	0.673 (0.213)	0.797 (0.106)		
Water	–0.525 (0.363)	0.779 (0.120)	0.878 (0.050)	0.856 (0.064)	0.551 (0.336)	
Bulk den.	0.436 (0.462)	–0.690 (0.197)	–0.815 (0.093)	–0.815 (0.093)	–0.631 (0.254)	**–0.936 (0.019)**

in *P. maritime* in combination with microphytobenthos biomass as a result of increased exposure time (Austen et al. 1999).

Stability Regulation: an Ecosystem Comparison

Significant spatial variation was observed in sediment stability between freshwater, estuarine mudflat, and estuarine saltmarsh sites. Stability was highest in the saltmarsh site and lowest in the shallow freshwater site. Sediment stability was observed to increase with depth in the freshwater sites and with distance up the shore in the estuarine sites. In general, sediment stability was higher in the estuary than it was in the lake. No significant correlations were observed between sediment stability and any of the measured variables across the five sites indicating stability regulation varies between sites or is controlled by variables not considered in this study (Table 3.3). One example of the former is the influence of electrostatic and physico-chemical particle-particle attractions that increase with sodium chloride concentration (i.e. salinity, Lerman 1979; Packman and Jerolmack 2004). Thus, cohesive aggregation increases across the salinity gradient such that estuarine sediments are more 'cohesive' than freshwater sediments. However, this would represent a sedimentological view and it is almost certain that extracellular polymers are also influenced by the ionic nature of their surrounding and contribute more to sediment cohesion under saline conditions. This hypothesis suggests that physico-chemical processes are the main drivers of sediment stability across ecosystem types with bio-physical and bio-chemical processes also being affected by the physicochemical changes. This also explains why, although levels of extracellular polymers are high in the deep freshwater sites, the enhanced stability is less than for the intertidal sites. This possibility requires further research.

Stability was significantly correlated with a number of variables within sites. The positive correlation between sediment stability regulation and colloidal carbohydrate concentration in the deep freshwater site was in agreement with conventional diatom biostabilization theory (e.g., Madsen et al. 1993; Paterson 1994). The absence of this relation in the shallow freshwater site may be the result of excessive wind mixing reducing microphytobenthos biomass, and hence the production of carbohydrates.

3.1.4 Conclusions

The variation in sediment stability was not explained by a single variable across ecosystems. Instead, stability was found to be system specific and therefore care must be taken when defining general rules of stability across ecosystem types. The stability of the bed was higher in the estuarine sites than it was in the freshwater system, probably as a result of increasing electrostatic effects on particle-particle attraction and polymer related adhesion. Stability was higher at 4.3 m overlying water depth compared to 2.1 m overlying water depth in the freshwater site most likely as a result of higher autotrophic production of carbohydrate concentration. Colloidal carbohydrate concentrations were higher in the freshwater ecosystem than in the estuarine ecosystem but less effective at stabilization.

Acknowledgments

We thank the organizers of the SEDYMO conference and acknowledge NERC Doctoral funding to Bryan Spears (NER/S/A/2003/11324) and James Saunders (NER/S/A/2003/11890). The authors acknowledge the support by the MarBEF Network of Excellence 'Marine Biodiversity and Ecosystem Functioning' which is funded by the Sustainable Development, Global Change and Ecosystems Programme of the European Community's Sixth Framework Programme (contract no. GOCE-CT-2003-505446). This publication is contribution number MPS-06056 for MarBEF.

References

Austin I, Andersen TJ, Edelvang K (1999) The influence of benthic diatoms and invertebrates on the erodibility of an intertidal mudflat, the Danish Wadden Sea. Estuarine and Coastal and Shelf Science 49:99–111

Benoy GA, Kalff J (1999) Sediment acuumulation and Pb burdens in submerged macrophyte beds. Limnology and Oceanography 44(4):1081–1090

Decho W (2000) Microbial biofilms in intertidal systems: an overview. Continental Shelf Research 20:1257–1273

Grady JR (1981) Properties of seagrass and sand flat sediments from the intertidal zone of St Andrews Bay, Florida. Estuaries 4(4):335–344

Goto N, Kawamura T, Mitamura O, Terai H (1999) Importance of extracellular organic carbon production in the total primary production by tidal-flat diatoms in comparison to phytoplankton. Marine Ecology Progress Series 190:289–295

Head RM, Jones RI, Bailey-Watts AE (1999) Vertical movements by planktonic cyanobacterial and the translocation of phosphorus: implications for lake restoration. Aquatic Conservation: Marine and Freshwater Ecosystems 9:111–120

Hilton J, Lishman P, Allen V (1986) The dominant processes of sediment distribution and focussing in a small, eutrophic, monomictic lake. Limnology and Oceanography 31:125–133

HIMOM (2005) Heirarchical Monitoring Methods. European commission fifth framework programme. Contract: EVK3-CT-2001-00052

Kenworthy WJ, Ziemen JC, Thayer GW (1982) Evidence for the influence of seagrasses on the benthic nitrogen cycle in a coastal plain estuary near Beaufort, North Carolina (USA). Oecologia 54(2):152–158

Lick W, Huang H (1993) Flocculation and the physical properties of flocs. In: Mehta AJ (ed) Nearshore and estuarine cohesive sediment transport. AGU, Washington, DC, pp 21–39

Lerman A (1979) Geochemical processes: water and sediment environments. John Wiley and Sons Publishers, New York

Madsen KN, Nilsson P, Sundbäck K (1993) The influence of benthic micro-algae on the stability of a subtidal sediment. Journal of Experimental Marine Biology and Ecology 170:159–177

Nedwell DB, Raffaelli DG (eds) (1999) Advances in Ecological Research Estuaries 29. Academic Press, San Diego, CA

Nedwell DB, Jickells TD, Trimmer M, Sanders R (1999) Nutrients in estuaries. In: Nedwell DB, Raffaelli DG (eds) Advances in Ecological Research: Estuaries 29. Academic Press, San Diego, CA

Packman AI, Jerolmack D (2004) The role of physicochemical processes in controlling sediment transport and deposition in turbidity currents. Marine Geology 204:1–9

Paterson DM (1989) Short-term changes in the erodibility of intertidal cohesive sediments related to the migratory behaviour of epipelic diatoms. Limnology and Oceanography 24:223–234

Paterson DM (1994) Microbiological mediation of sediment structure and behaviour. In: Stal LJ, Caumette P (eds) Microbial Mats. NATO ASI Series vol. G35, Springer-Verlag, Berlin Heidelberg

Paterson DM (1997) Biological mediation of sediment erodibility, ecology and physical dynamics. In: Burt N, Parker R, Watts I (eds) Cohesive Sediments. pp 215–229, Wiley Interscience, Chichester

Paterson DM, Black KS (1999) Water flow, sediment dynamics, and benthic biology. In: Raffaelii D, Nedwell D (eds) Advances in Ecological Research. pp 155–193, Oxford University Press, Oxford
Perkins RG, Honeywill C, Consalvey M, Austin HA, Tolhurst TJ, Paterson DM (2003) Changes in microphytobenthic chlorophyll a and EPS resulting from sediment compaction due to de-watering: opposing patterns in concentration and content. Continental Shelf Research 23:575–586
Tolhurst TJ (1999) Microbial mediation of intertidal sediment erosion. Ph.D. thesis. University of St Andrews
Tolhurst TJ, Black KS, Paterson DM, Mitchener H, Termaat R, Shayler SA (2000) A comparison and measurement standardisation of four in situ devices for determining the erosion sheer stress of intertidal sediments. Continental Shelf Research 20:1397–1418
Underwood GJC, Paterson DM, Parkes RJ (1995) The measurement of microbial carbohydrate exopolymers from intertidal sediments. Limnology and Oceanography 40:1243–1253
Weyenmeyer GA, Meili M, Pierson DC (1995) A simple method to quantify sources of settling particles in lakes: resuspension versus new sedimentation of material from planktonic production. Marine and Freshwater Research 46:223–231
Yallop ML, Paterson DM, Wellsbury P (2000) Interrelationships between rates of microbial production, exopolymer production, microbial biomass and sediment stability in biofilms of intertidal sediments. Microbial Ecology 39:116–127

Sabine Ulrike Gerbersdorf · Thomas Jancke · Bernhard Westrich

3.2 Determination of Sediment Stability by Its Physico-Chemical and Biological Properties: Considering Temporal and Vertical Gradients at Different Contaminated Riverine Sites

3.2.1 Introduction

In the past, hazardous contaminants were discharged in large quantities into water bodies where they subsequently accumulated within the bottom sediments. This legacy of the past is found world-wide in rivers, lakes, harbors, estuaries and near-shore areas which are often buried at depths of up to several meters (summarized in Foerstner et al. 2004; Ziegler 2002). However, under certain hydraulic conditions, these former immobilized contaminants might be eroded and become bioavailable and toxic. To prevent ecological disasters and to achieve a good ecological status of the aquatic habitats, as required in the Water Framework (2000/60/EC) Directive, the potential erosion risk of areas of concern has to be evaluated to recommend further treatments such as remediation or sub-aqueous capping. Although several contaminated riverine sites and lakes have been investigated for their sediment erosion behavior world-wide (Ziegler 2002), only a few studies are known from German rivers with emphasis on sediment stability (Haag et al. 2001). In this context, most studies concentrated on the physico-chemical sediment properties such as bulk density, particle size classes and mineralogy that are characterizing erosion resistance (Jepsen et al. 1997; McNeil and Lick 2004). Over the last years, the biogenic mediation of sediment erosion has received increasing attention, namely through stabilizing effects by the mucilaginous matrix of extracellular polymeric substances (EPS) produced by macrofauna, microalgae and bacteria (de Brouwer et al. 2000; de Deckere et al. 2001; Flemming and Wingender 2001). However, it is still rare that physico-chemical *and* biological sediment properties are investigated simultaneously with regard to sediment stability, and only a few properties are generally considered in total (de Brouwer et al. 2000). Considering biostabilization,

most investigations originate from tidal flats and thus concentrate on biofilms at the sediment surface with a focus on microalgae as the main producers of EPS. However, bacteria are also known to excrete significant amounts of polymeric substances such as carbohydrates as well as proteins (Flemming and Wingender 2001), and the bacterial production is likely to dominate in deeper sediment layers below the biofilm/photic zone. So far, studies on bacterial biomass and bacterial EPS production have not been related to sediment stability. Hence, the present study aimed to determine a wide range not only of physico-chemical (water content, organic content, grain size, cation exchange capacity, liquid and plastic limits, bulk density) but also biological parameters including macrofauna abundance, microalgal biomass, bacterial cell numbers and EPS fractions (water- and resin-soluble carbohydrates and proteins). Covariance pattern of the different sediment properties were considered by simultaneously sampling and statistical evaluation. In parallel, the critical erosion shear stress for mass erosion was determined in a rectangular pressure duct called the SETEG (*S*trömungskanal zur *E*rmittlung der *t*iefenabhängigen *E*rosionsstabilität von *G*ewässersedimenten) system (Kern et al. 1999). Hence, master-variables for a reliable, efficient and economically viable erosion risk assessment of contaminated riverine sites can be derived. The transferability of the data obtained was addressed by including spatial (different sampling sites) and temporal (different seasons) gradients. Since the erosion properties of sediments may vary in a non-uniform and non-predictable manner as a function of depth, the present study investigated sediment stability and its sediment properties within natural sediments spanning the zone between surface and 50 cm depth.

3.2.2 Material and Methods

Site description. The lock-regulated river Neckar is a major tributary to the river Rhine, draining a highly industrialized and agrarian affected catchment area of about 14 000 km^2 in the Southwest of Germany. Sediment samples were taken in the reservoirs of Deiziau (km 200), Hofen (km 176), Poppenweiler (km 165) and Lauffen (km 137), near-bank in a water depth of less than 2 m. These study sites are known for their high sediment contamination with heavy metals and polychlorinated biphenyls as well as organic stannous compounds (Haag et al. 2001). The Iffezheim barrage is located in the river Rhine (catchment area of 165 000 km^2) at km 334. Sediments were withdrawn in front of the weir section in a water depth of around 2 m. The sediments of this reservoir are heavily contaminated with hexachlorobenzene (HCB, Zipperle and Deventer 2003). At the river Elbe (catchment area of 148 268 km^2), sampling took place at water depths of 1–2.5 m in front of the weir section (Pœlouc, Czech site, km 223) and in the center of groyne fields: Coswig (km 235), Stecky (km 280), Magdeburg (km 318), Fahlberg-List (km 319), Havelberg (km 419) and Hamburg (km 607). The groyne fields are polluted with heavy metals and arsenic originating from mines by the discharge of the tributary rivers Mulde and Saale (Foerstner et al. 2004). Sampling campaigns took place in different seasons: Deizisau, Hofen, Poppenweiler: April, June, September 2004; Lauffen: January–December 2003 (river Neckar); Iffezheim: March 2004 (river Rhine); Prelouc: April 2005; Coswig, Steckby: June 2005; Fahlberg-List: June, August, November 2005; Magdeburg, Havelberg, Hamburg: August 2003 (river Elbe).

Sampling and proceeding. At each study site, sediment samples were withdrawn using two sizes of cylindrical coring tubes of 150/100 cm in length and 13.5/11 cm inner diameter, respectively. The first two sediment cores were used to determine bulk density non-intrusively by a gamma-ray densitometer (Dreher 1997) as well as the critical shear stress for mass erosion in the rectangular pressurized SETEG-flume (Kern et al. 1999; Haag et al. 2001) in cm steps to depths of usually 50 cm. Two more sediment cores with similar bulk density profiles were sectioned into different layers at intervals of 0.5–2 cm and the appropriate layers from both cores were pooled and mixed thoroughly to overcome intrinsic patchiness. The sediment properties were determined within each of these layers. The fifth sediment core was used for sieving the top 10 cm sediment by a 500 μm mesh sieve, retaining all organisms which are referred to as macrofauna.

Sediment properties. The following physico-chemical sediment properties were determined: *water content*, *mineral composition, soil particle size classes* (sand 2–0.063 mm, silt 0.002–0.063 mm, clay <0.002 mm), *TOC* (*t*otal *o*rganic *c*arbon), *CEC* (*c*ation *e*xchange *c*apacity), *liquid* and *plastic limits*. The biological sediment properties included: abundances of *macroinvertebrates*, concentrations and content of *chlorophyll a* (proxy for algal biomass) and *pheopigments* (indicator for degraded microalgal pigments*), bacterial cell numbers* (DAPI staining, Epifluorescence Microscope) and *EPS* (*e*xtracellular *p*olymeric *s*ubstances) fractions. Briefly, EPS were extracted from dried and homogenized sediment samples over a fixed period with distilled water as well as with CER (*c*ation *e*xchange *r*esin), modified after de Brouwer and Stal 2001; Frølund et al. 1996. Within the supernatants, the water-extractable (colloidal) carbohydrates, the CER-extractable carbohydrates as well as the CER-extractable proteins – corrected for humic acids – were determined spectrophotometrically (protocols in Frølund et al. 1996). In pre-experiments, the extraction procedure was optimized regarding the yield and ratio of the different EPS fractions by varying extractants, extracting volume and sediment dry weights. For more details on the determination of sediment properties, especially the EPS fractions see also Gerbersdorf et al. (2005).

Statistics. Multivariate Statistics, PCA (*P*rincipal *C*omponent *A*nalysis), was conducted by SPSS 12.0 for Windows to address the covariance pattern of the physico-chemical and biological sediment properties and their impact on sediment stability (Haag and Westrich 2002). For more details see also Gerbersdorf et al. (2005).

3.2.3 Results and Discussion

Sediment stability – vertical profiles of $\tau_{crit.\,E}$ and ρ. On the basis of bulk density profiles, horizons of differing consolidation and particles sizes could be selected. Using this data it was ensured, that the appropriate horizons of replicate sediment cores were pooled after sectioning. At the sediment surface of all stations, the bulk density was relatively low (1.1–1.3 g cm^{-3}) along with high water content (up to 71%) (Fig. 3.4). Although the bulk density tended to increase towards deeper sediment layers, in most cases, clear consolidation effects could not be visualized in the top 25 cm. Pronounced

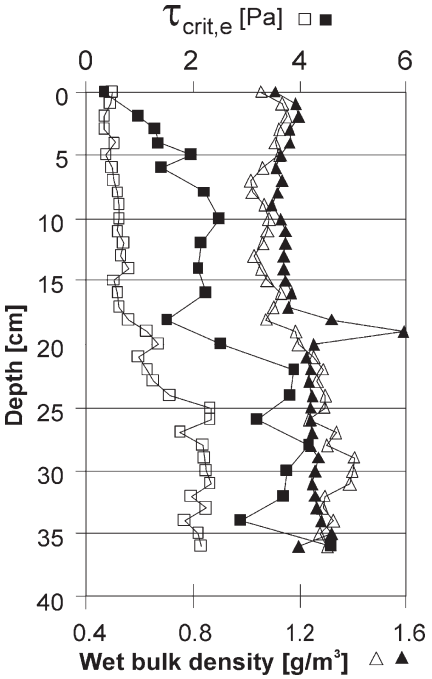

Fig. 3.4.
Vertical depths profiles of critical erosion shear stress ($\tau_{crit.\,E}$, squares) and wet bulk density (ρ, *triangles*), examples shown for Prelouc reservoir (*open symbols*) and Fahlberg groyne field (*black symbols*), April and June 2005, respectively

peaks of bulk density values usually corresponded to sandy horizons along with low organic content and decreasing sediment stability (e.g., 18 cm depth, Fahlberg, Fig. 3.4). The critical shear stress determined within the top 25 cm sediment by the SETEG flume, were also relatively low at all reservoirs (mostly below 1 Pascal (Pa), range of 0.3–2.9 Pa, Table 3.4, Fig. 3.4) in accordance with data from active sedimentation/resuspension areas such as the intertidal flats (0.13–1.0 Pa, Austen and Witte 2000). Although older, more consolidated horizons showed higher critical shear stress values compared to younger, freshly deposited sediment layers on top, the stability of all horizons was surprisingly low. The measured critical shear stress of the sediments was opposed to different scenarios of naturally occurring bottom shear stress, for instance calculated by the 1-D flow and transport model COSMOS for the Lauffen Reservoir/river Neckar (Kern 1997). Thus, it was indicated that a three to five fold mean discharge (around 500 $m^3\,s^{-1}$ instead of 80 $m^3\,s^{-1}$) would erode the top 25 cm sediment layers with shear stress values of 1–2.5 Pa and a five years flood event (corresponds to 9 Pa) could remove all sediments at depths below 50 cm (Haag et al. 2001). Haag et al. (2001) detected polluted sediment layers in the Lauffen Reservoir/river Neckar at only 20–70 cm depth but some contaminations were even directly located at the sediment surface due to local heterogeneity in erosion/deposition pattern. Chemical and ecotoxicological studies revealed the occurrence and bioavailability of contaminations within the top 15 cm sediment at different study sites in river Neckar and Rhine (Zipperle and Deventer 2003). Thus, the risk of erosion was severe at the contaminated reservoirs of river Neckar, even under moderate bottom shear stresses. The same applies for the study sites of river Rhine and Elbe (data not discussed).

Table 3.4.
Mean values of critical shear stress (Pa) given for different study sites and at different depths

	$\tau_{crit.E}$ (Pa)		
	Surface	1–5 cm	16–20 cm
Deizisau	0.52	0.61	0.70
Hofen	0.45	0.59	0.86
Poppenweiler	0.64	0.64	1.04
Lauffen	0.69	1.07	1.67
Iffezheim	0.38	0.44	0.78
Prelouc	0.47	0.41	0.90
Coswig	0.28	0.40	8.40
Steckby	0.33	8.90	8.90
Fahlberg	0.44	1.11	4.85
Magdeburg	0.80	0.66	0.43
Havelberg	0.52	0.72	2.50

Biogenic Mediation of Sediment Stability

Macrofauna. The impact of macroorganisms on sediment stability can be negative due to bioturbation and grazing activities but we could not prove such an effect in the present study. On the other hand, certain worms and midge larvae such as *Tubificidae* and *Chironomidae* are known to live in tubes which act as sediment traps and which are coated with polymeric substances (Datry et al. 2003; Olafsson and Paterson 2004). For all river Neckar data ($n = 21$), a positive relation between the critical shear stress values and the abundances of *Tubificidae* (Pearson's $r = 0.63$) as well as *Chironomidae* (Pearson's $r = 0.61$) could be shown for the top 10 cm sediment. Since there were no correlation between polymeric substances and macrozoobenthos abundance, the tubes itself must have contributed to sediment stabilization. It remains to be investigated, which proportion of biostabilization might be due to macrofauna tubes formation, when compared to other biological impact factors like EPS produced by microalgae and bacteria.

Microalgae. At all riverine sites, especially within the groyne fields, the turbidity and light attenuation ($k = 2$–$3\ m^{-1}$) within the water column was high, calculated by vertical underwater light profiles. However, the resulting light regime at the sediment surface (minimum range 8–30 $\mu E\ m^{-2}\ s^{-1}$) still allowed photosynthetic activity by benthic microalgae and thus, possible EPS excretion (Smith and Underwood 2000). Microscopy revealed the occurrence and dominance of benthic diatoms (Bacillariophyceae, Pennales), and around 70 species were determined in total at all sites (Gerbersdorf et al. unpubl.). In the sediments of the reservoirs, only a few deposited phytoplankton species were found. In the groyne fields sediments, pelagic diatoms (Bacillariophyceae, Centrales) and pelagic green algae (Chlorophyta, Chlorococcales/Chlorellales) were more dominant, thereby reflecting the two main components of the phytoplankton in the river Elbe (Gerbersdorf et al. unpubl.). Presumably the deposited pelagic species contrib-

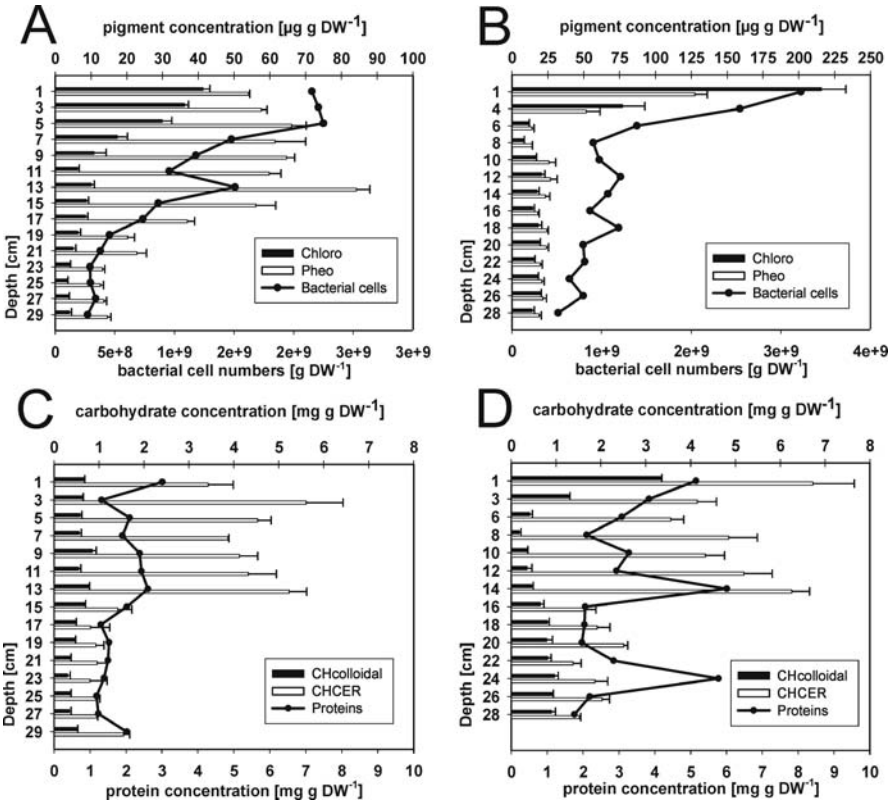

Fig. 3.5. Vertical depth profiles of chlorophyll *a* (*black bars*), pheopigment (*white bars*), bacterial cell numbers (*black line with circles*) (*A* and *B*) and polymeric substances such as colloidal carbohydrates (*black bars*), resin-extractable carbohydrates (*white bars*) and proteins (*black line with circles*) (*C* and *D*). Examples shown for Prelouc reservoir (*A* and *C*) as well as for the Fahlberg groyne field (*B* and *D*), April and June 2005, respectively

uted considerably to the chlorophyll *a* concentration in the sediments indicated by higher microalgal biomass in the groyne fields (river Elbe: Fahlberg 24, UFZ Magdeburg 36, Havelberg 75, Hamburg 60), compared to the reservoirs (river Neckar: Deizisau 27, Hofen 9, Poppenweiler 12, Lauffen 12, river Elbe: Prelouc 11) (µg cm^{-3}), mean value of surface, fresh sediment, Fig. 3.5a and b). Still, the microalgal biomass in all riverine sediments investigated was surprisingly high and even in the range of highly photosynthetic active habitats such as intertidal flats or tidal sandy beaches (de Brouwer and Stal 2001).

Bacteria. Similar to the vertical distribution of the microalgal biomass, the bacterial cell numbers were highest in the top sediment layers and decreased over depth (Fig. 3.5a and b). This indicates the well-known mutual profit of bacteria and microalgae by their excudates (Yallop et al. 2000). The bacterial cell numbers within the sediment surface ranged from $4–9 \times 10^8$ bacterial cells cm^{-3} fresh sediment at all study sites.

EPS fractions. The concentrations of water-extractable (colloidal) carbohydrates in the sediment surface layer were in the range of 0.11–0.49 mg g DW^{-1} with maximum values of 1.52 and 1.82 mg g DW^{-1} (groyne field Hamburg and Havelberg/river Elbe, respectively) and 2.37 mg g DW^{-1} (Deizisau Reservoir/river Neckar). While the colloidal carbohydrates represented only about 10% of the total carbohydrate pool in most reservoirs (exception Deizisau: 20–40%), their contribution was much higher in the groyne fields (9–59%, mostly around 30%, Fig. 3.5c and d). Although the concentrations of colloidal carbohydrates seemed low at first, they were well in the range of data known from pronounced biofilms with high photosynthetic activity and EPS excretion (de Brouwer et al. 2000). The concentrations of proteins in the sediment surface layer were similar to the CER-extractable carbohydrates and mostly in the range of 1.80–5.15 mg g DW^{-1} with some higher values in the reservoirs of the river Neckar (Deizisau 12.90, Hofen 9.60 and Poppenweiler 10.20 (mg g DW^{-1})). Thus, the quantity of polymeric substances could be sufficient to have a significant impact on sediment stability.

Which organisms are excreting polymeric substances? Microalgae are known to produce significant amounts of carbohydrates (Underwood et al. 2004), while bacteria could excrete additionally proteins (Flemming and Wingender 2001). Plotting the data from all study sites at all seasons together, excretion of colloidal and CER-extractable carbohydrates as well as proteins by microalgae and by bacteria, could be shown at all depths (except for the sediment surface, no relation of bacteria and protein, Table 3.5). The positive relation of pheopigments and polymeric substances hints towards the release of EPS from senescent algal material (Table 3.5).

Table 3.5. Potential EPS producers (*Chlorophyll a* as proxy for microalgal biomass, *Pheophytin* as proxy for microalgal degradation products, *Bacteria* = bacterial cell numbers) versus EPS components (*CH colloidal* = water-extractable Carbohydrates, *CH CER* = resin-extractable carbohydrates, proteins) and their relation to water content. The correlation coefficients are given for the top layers (*Surface*, 0.5 cm) and deeper layers (*Deep*, to depth of 10 cm). The different significance levels are indicated by $p < 0.05$ (a) and $p < 0.001$ (b) for Pearson's *r*

	Water Content		Chlorophyll *a*		Pheophytin		Bacteria	
	Surface	Deep	Surface	Deep	Surface	Deep	Surface	Deep
Chlorophyll *a*	0.81[b]	0.76[b]						
Pheophytin	0.96[b]	0.88[b]	0.77[b]	0.79[b]				
Bacteria	0.92[b]	0.57[b]	0.53[a]	0.58[b]	0.55[a]	0.34[b]		
CH colloidal	0.68[b]	0.72[b]	0.62[b]	0.57[b]	0.69[b]	0.73[b]	0.66[b]	0.25[a]
CH CER	0.41	0.45[b]	0.45[a]	0.46[b]	0.17	0.39[b]	0.48	0.37[b]
Proteins	0.17	–0.11	0.53[b]	0.13	0.41[a]	–0.06	0.01	0.11

[a] $p < 0.05$.
[b] $p < 0.001$.

Correlation of sediment stability and sediment properties

Physico-chemical properties. The critical shear stress showed positive relations with the clay and silt fraction (<63 µm), as well as with TOC and CEC (Table 3.6, Gerbersdorf et al. 2005, 2007). Along with decreasing grain size, the cation exchange capacity (CEC) is increased due to the enhanced number of active adsorption sites in fine-grained sediments. In muddy sediments, the organic content is much higher compared to quartz sand, and these polymeric compounds with active binding sites will add to sediment stability by adsorption to the small particles (de Brouwer et al. 2000). Moreover, the sediment will consolidate over time and depth (Table 3.4), mostly a dewatering effect (Perkins et al. 2003), which is often reflected in increasing bulk densities. In the present data set, sandy layers with high bulk density and low erosion resistance were not excluded from the data set. Accordingly, the relation between critical shear stress and bulk density as well as water content showed some inherent pattern (Table 3.6). Usually, the shear stress was positively correlated with bulk density (e.g., 0.65, $p < 0.001$ for top layers of Fahlberg), while the relation with water content was inverse as could be shown for the top 10 cm sediment from the groyne field Fahlberg (Table 3.6).

Table 3.6. Critical shear stress versus sediment properties (*CH colloidal* = water-extractable Carbohydrates, *CH CER* = resin-extractable Carbohydrates, $d < 63$ µm = grain sizes, *TOC* = Total Organic Carbon, *CEC* = Cation Exchange Capacity). The correlation coefficients are given for the upper layers (*Top*, from surface to 10 cm depth) as well as for deeper layers (*Deep*, below depths of 10 cm), shown exemplary for one reservoir (Lauffen, River Neckar) and one groyne field (Fahlberg, River Elbe). The significance levels are indicated by $p < 0.05$ (a) and $p < 0.001$ (b) for Pearson's *r*

	Lauffen reservoir		Fahlberg groyne field	
	Top	Deep	Top	Deep
Chlorophyll *a*	–0.45	0.20	–0.45	0.09
Pheophytin	–0.08	0.11	–0.57[a]	0.24
Bacteria	–0.95[b]	–0.19	–0.44	0.10
CH colloidal	0.30	0.54[b]	–0.63[a]	0.54[a]
CH CER	0.02	0.44[a]	0.73[b]	0.02
Proteins	0.33	0.43[a]	–0.21	0.43[a]
Bulk density	0.38	–0.49[b]	0.65[b]	–0.08
Water content	–0.57	0.29	–0.65[b]	0.29
$d < 63$ µm	0.49	0.68[b]	0.41	0.30
TOC	–0.34	0.23	–0.10	0.53[b]
CEC	0.91[a]	0.35	0.30	0.49[a]
Depth	0.53[a]	0.56[b]	0.85[b]	0.48[a]

[a] $p < 0.05$.
[b] $p < 0.001$.

Biological properties. The interrelations between the critical shear stress of erosion and the microorganisms as well as their excreted EPS components have been highly variable in spatial, temporal and vertical terms (see also Gerbersdorf et al. 2005, 2006a,b). At times of high photosynthetic/metabolic activity, huge concentrations of polymeric substances were produced in the top sediment layers, closely related to the biomass of their producers: microalgae and bacteria (Table 3.5). Plotting sediment surface (0–0.5 cm) data from different study sites and seasons together, positive relations between the sediment stability and microalgal/bacterial biomass (Pearson's $r = 0.28 / 0.42$) as well as the resin-extractable carbohydrates (Pearson's $r = 0.44$) could be ruled out (Gerbersdorf et al. 2006b). With depth, the biomass of the microorganisms as well as their excretion products were decreasing (Fig. 3.5a and b) while sediment stability was increasing, resulting in some negative interrelations within the top sediment layers (Table 3.6). In deeper layers, a positive relation between all biologically produced EPS components and sediment stability could be ruled out, independent of the biomass of the EPS producers (Table 3.6, Yallop et al. 2000). Migratory activity of buried microalgae might have maintained the pool of polymeric substances by permanent excretion of colloidal carbohydrates during movements (de Brouwer and Stal 2002; Underwood et al. 2004). Secondly, the bacterial EPS production might have gained more and more importance in layers below the photic zone. However, increasing ratios of carbohydrates and proteins over microorganisms biomass indicated rather irreversible binding of the biologically produced polymeric material to sediment particles and thus, accumulation over depth. Although it is known that colloidal carbohydrates are easily dissolved in water, the large adsorptive surface area in fine-grained sediments might retain even loosely bound carbohydrates, followed by a possible conversion into stronger attached fractions (de Brouwer et al. 2000). Consequently, not only the more recalcitrant CER carbohydrates with higher partition coefficient (indicating higher adsorption to sediment particles, de Brouwer and Stal 2001), but also the colloidal carbohydrates as well as proteins (presumably exoenzymes, Flemming and Wingender 2001) accumulate over depth or in distinctive sediment horizons. Presumably, the variations in the relation between biological properties and sediment stability were not only due to different quantities at the different study sites, seasons or depth (Table 3.6). The quality of the polymeric substances might also be crucial for binding sediment particles (Gerbersdorf et al. 2005). The quantity as well as the stabilizing potential of EPS might vary due to the physiological status and the taxonomic composition of their producers, influenced by abiotic parameters such as nutrients and light (de Brouwer and Stal 2001; Smith and Underwood 2000).

Combined influence of sediment properties on sediment stability. Although the correlations between the critical shear stress and single sediment properties have been significant, the correlation coefficients were low (up to 0.54 only, Table 3.6). Hence, PCA (Principal Component Analysis) was conducted in order to assess the covariance pattern of the sediment properties and their impact on sediment stability. Due to the high variability of the biological data, this multivariate statistic approach was performed for limited data sets of similar origin (e.g., study site, season): Lauffen January–December 2003, Deizisau/Hofen/Poppenweiler April 2004 (river Neckar), Fahlberg June–November 2005 (river Elbe). All other study sites were sampled only once, thus their data

set was too small to conduct PCA. Congruently, the combined influence of grain size, TOC, CEC and polymeric substances, constituting the interparticle forces, was most important for sediment stability. In all cases, the critical shear stress correlated best to the main components in which these appropriate sediment properties were combined. Thereby, the magnitude of the correlation coefficient was significantly enhanced compared to the correlations between shear stress and single sediment properties only. The correlation coefficients applying the PCA approach were $R = 0.88$ for Lauffen (Gerbersdorf et al. 2005), $R = 0.70$ and 0.91 for Deizisau, Hofen, Poppenweiler (Gerbersdorf et al. 2007) and $R = 0.81$ for Fahlberg (biplot of critical shear stress to main component I in Table 3.7, biplot not shown).

3.2.4 Conclusions

The present study evaluated the covariance pattern of physico-chemical and biological sediment properties and their impact on sediment stability, investigating natural sediments from contaminated riverine sites over depth. Biogenic mediation was mainly due to the mucilaginous matrix of extracellular polymeric substances (EPS), excreted by microalgae and bacteria. These polymeric substances such as proteins and carbohydrates contributed significantly to the inter-particle forces, along with grain size, TOC (total organic carbon) and CEC (cation exchange capacity). This interplay between fine-grained sediment, offering high binding capacities and charge densities, as

Table 3.7.
Loading matrix showing three extracted main components (= vectors, vertical) explaining 39%, 21% and 17% of the variance in the data set, respectively. The loadings corresponds to Pearson's *r* and loadings > 0.35 ($n < 200$) are considered to be significant (*Chlorophyll a* as proxy for microalgal biomass, *Pheophytin* as proxy for microalgal degradation product, *Bacteria* = bacterial cell numbers, *CH colloidal* = water-extractable carbohydrates, *CH CER* = resin-extractable carbohydrates, *TOC* = Total Organic Carbon, *CEC* = Cation Exchange Capacity)

	Component		
	1	2	3
Chlorophyll *a*	0.917	0.235	0.038
Pheophytin	0.890	0.016	0.113
Bacteria	0.173	0.233	0.722
Protein	0.486	0.068	0.344
CH colloidal	0.317	0.524	–0.494
CH CER	0.232	0.075	0.872
Bulk density	–0.561	–0.241	0.540
Water content	0.908	0.136	0.064
Clay	0.477	0.706	–0.154
Silt	–0.113	0.897	0.135
Sand	–0.189	–0.961	–0.007
TOC	0.832	0.074	–0.271
CEC	0.181	0.181	–0.651
Depth	0.559	0.307	–0.485

well as polymeric substances, permeating the void space and coating particles with their active binding sites, is most crucial for erosion resistance. Hence, the influence of both, physico-chemical *and* biological properties could be shown, even over depth, where mostly sedimentological impact was considered before. This overall sediment protection by particle-organisms interaction may be more effective in resisting erosion forces than pronounced surface biofilms, which have been the focus of investigations so far. In assessing the collective influence of sedimentological and biological properties, a better correlation between sediment stability and the master-variables could be achieved in comparison to single correlations. The need for such a comprehensive risk assessment of contaminated riverine sites became again evident in the present study, because at all study sites, low erosion resistance was determined within the sediments to depths of 50 cm. Compared to naturally occurring bottom shear stress, a severe erosion risk of these polluted sediment horizons could be established, even for medium-energy events.

Acknowledgments

The authors would like to thank for their enthusiastic and excellent support: J. Stork and the crew of 'Max Honsell' (sampling facilities); T. Eder, T. Fimpel, R. Ninov (EPS determination); T. Basta, M. Eder, A. Kuhm, W. Wen (bacterial cell numbers); L. Taeuscher, U. Mueller (microalgae species composition) and I. Haag (statistics). The investigations presented here were part of the project SEDYMO, (*Se*diment *Dy*namic and *Mo*bility) funded by the German Federal Ministry of Education and Research (BMBF).

References

Austen I, Witte G (2000) Comparison of the erosion shear stress of oxic and anoxic sediments in the East Frisian Wadden Sea. In: Flemming BW, Delafontaine MT, Liebezeit G (eds) Muddy coast dynamics and resource management, Proc Mar Sci, vol. 2. Elsevier, Amsterdam, pp 75–84

Datry T, Malard F, Niederreiter R, Gibert J (2003) Video-logging for examining biogenic structures in deep heterogeneous subsurface sediments. C. R. Biologies 326:589–597

De Brouwer JFC, Stal LJ (2001) Short-term dynamics in microphytobenthos distribution and associated extracellular carbohydrates in surface sediments of and intertidal mudflat. Mar Ecol Prog Ser 218:33–44

De Brouwer JFC, Stal LJ (2002) Daily fluctuations of exopolymers in cultures of benthic diatoms *Cylindrotheca closterium* and *Nitzschia sp.* (Bacillariophyceae). J Phycol 38:464–472

De Brouwer JFC, Bjelic S, de Deckere, EMGT, Stal, LJ (2000) Interplay between biology and sedimentology in a mudflat (Biezelingse Ham, Westerschelde, The Netherlands). Cont Shelf Res 20:1159–1177

De Deckere EMGT, Tolhurst TJ, de Brouwer JFC (2001) Destabilisation of cohesive intertidal sediments by infauna. Estuar Coast Shelf Sci 56:665–669

Dreher T (1997) Non intrusive measurement of particle concentration and experimental characterization of sedimentation. Sonderforschungsbericht 404, Universitaet Stuttgart

Flemming HC, Wingender J (2001) Relevance of microbial extracellular polymeric substances (EPS) – Part I: Structural and ecological aspects. Water Sci Technol 43(6):1–8

Foerstner U, Heise S, Schwartz R, Westrich B, Ahlf W (2004) Historical Contaminated Sediments and Soils at the River Basin Scale. J Soil and Sediments 4:247–260

Frølund B, Palmgren R, Keiding K, Nielsen PH (1996) Extraction of extracellular polymers from activated sludge using a cation exchange resin. Wat Res 30:1749–1758

Gerbersdorf SU, Jancke T, Westrich B (2005) Physico-chemical and biological sediment properties determining erosion resistance of contaminated riverine sediments – temporal and vertical pattern at the Lauffen reservoir / river Neckar, Germany. Limnologica 35:132–144
Gerbersdorf SU, Jancke T, Westrich B (2007) Sediment properties for assessing the erosion risk of contaminated riverine sites. Journal of Soils and Sediments: 7(1):25–35
Haag I, Westrich B (2002) Process governing river water quality identified by principal component analysis. Hydrol Process 16:3113–3130
Haag I, Kern U, Westrich B (2001) Erosion investigation and sediment quality measurements for a comprehensive risk assessment of contaminated sediments. Sci Total Environ 266:249–257
Jepsen R, Roberts J, Lick W (1997) Effects of bulk density on sediment erosion rates. Water Air Soil Poll 99:21–31
Kern U (1997) Transport von Schweb- und Schadstoffen in staugeregelten Fließgewaessern am Beispiel des Neckars. Mitteilungen des Instituts fuer Wasserbau 93. Universitaet Stuttgart
Kern U, Schuerlein V, Holzwarth M, Haag I, Westrich B (1999) Ein Strömungskanal zur Ermittlung der tiefenabhängigen Erosionsstabilität von Gewässersedimenten: das SETEG-System. Wasserwirtschaft 89:72–77
McNeil J, Lick W (2004) Erosion rates and bulk properties of sediments from the Kalamazoo River. J Great Lakes Res 30:407–418
Olafsson JS, Paterson DM (2004) Alteration of biogenic structure and physical properties by tube-building chironomid larvae in cohesive sediments. Aquatic Ecology 38:219–229
Perkins RG, Honeywill C, Consalvey M, Austin HA, Tolhurst TJ, Paterson DM (2003) Changes in microphytobenthic chlorophyll *a* and EPS resulting from sediment compaction due to de-watering: opposing patterns in concentration and content. Cont Shelf Re 23:575–586
Smith DJ, Underwood GJC (2000) The production of extracellular carbohydrates by estuarine benthic diatoms: the effects of growth phase and light and dark treatment. J Phycol 36:321–333
Underwood GJC, Boulcott M, Raines CA, Waldron K (2004) Environmental effects on exopolymer production by marine benthic diatoms: dynamics, changes in composition, and pathways of production. J Phycol 40:293–304
Yallop ML, Paterson DM, Wellsbury P (2000) Interrelationships between Rates of Microbial Production, Exopolymer Production, Microbial Biomass, and Sediment Stability in Biofilms of Intertidal Sediments. Microb Ecol 39:116–127
Ziegler CK (2002) Evaluating sediment stability at sites of historic contamination. Environ Manage 29:409–427
Zipperle J, Deventer K (2003) Wirkungsbezogene Sedimentuntersuchungen zur Ableitung von Qualitätsmerkmalen und Handlungsempfehlungen, Teilprojekt 1: Entwicklung und Erprobung einer Strategie zur Beurteilung der Sedimentbeschaffenheit auf der Basis von Wirktests. LFU Karlsruhe

Volker Müller · Andreas Seibel · Dogan Kisacik · Giselher Gust

3.3 Simulation of Water Column Hydrodynamics by Benthic Chambers

3.3.1 Introduction

Water quality in coastal and inland water depends mainly on pollutant mobilization and dispersal. The processes of changing water quality are closely connected to the dynamics of fine sediments. Therefore the understanding of water quality requires a deeper insight in the processes of erosion, transport, deposition and consolidation of particulate matter under various physical, chemically and biologically conditions. Not ignoring the importance of chemical and biological controlled dynamics of particulate matter, it is obvious that all processes determining the water quality basically are affected by hydrodynamics.

Laboratory tests of the various interlinked processes of water quality dynamics are better reproduced under hydrodynamic conditions equivalent to the natural environment. These tasks call for a suite of different experimental devices to reproduce the

specific hydrodynamic conditions *(a)* in the benthic zone as well as *(b)* in the water body. In principle, a set of different experimental devices exist to fulfill the specific hydrodynamic conditions in these regions. With most of these only a single hydrodynamic parameter, considered as the most important one, for a selected sedimentological, chemical or biological process can be well controlled.

Within the SEDYMO project we developed an experimental apparatus to control more than one hydrodynamic parameter which affect processes on the benthic zone and in the water body occurring synchronously. The main task for the *B*enthic-*W*ater-*C*olumn-*S*imulator (BWCS) was the ability to perform investigations on the full cycle of erosion, transportation, deposition and consolidation of fine sediments at different physical, chemical and biological loading. Here the design and main characteristic of the BWCS are presented. BWCSs or the parent system – the Gust microcosm (Gust and Müller 1997; Tengberg et al. 2004) – were used for various projects within SEDYMO and the reader is referred to the corresponding contributions (Kleeberg 2006; Paterson 2006; Siepmann 2006).

3.3.2 Design of the Benthic Water-Column-Simulator

The design of the BWCS is determined by the requirement to control the most important hydrodynamic parameter for small scale processes occurring in the benthic zone as well as the most important hydrodynamic parameter controlling small scale processes in the pelagic region. In the benthic zone where exchange processes of particles and solutes at the interface between the fluid and the bed are dominant, the dynamic flow characteristics of the boundary layer are most relevant although the hydrostatic pressure is also important. For an equilibrium boundary layer flow, the most important hydrodynamic parameter is the bottom shear stress τ_b. For chemical and/or particulate reactions in the pelagic flow field then turbulence, characterized by u' (= RMS velocity) or, assuming isotropy, the turbulent kinetic energy (TKE)

$$\mathrm{TKE} = \frac{3}{2}u'^2 \tag{3.1}$$

is the most important hydrodynamic parameter.

A review of the existing erosion devices, channels or flow chambers (Brunk et al. 1996; Gust and Müller 1997; Tengberg et al. 2004) shows that in most cases either the bottom shear stress or the flow turbulence is well controlled. The principles of flow generation used in these different devices to adjust the hydrodynamic parameters are of various kind. Rotating disks, cylinders or special shaped bodies are mostly used for generating the desired values of bottom stress. For generating turbulence in the pelagic zone, moving grids or rotating paddle systems are used. But sometimes these systems are also used for generating bottom stress and vise versa. The Gust microcosm (rotating disk with central suction) and the EROMES system (propeller system) are widely used devices with a long history of investigation (Gust 1990; Müller et al. 1995; Gust and Müller 1997). A combination of these two systems could establish an experimental apparatus which allows the control of mean flow, bottom stress and flow turbulence within the same experimental system.

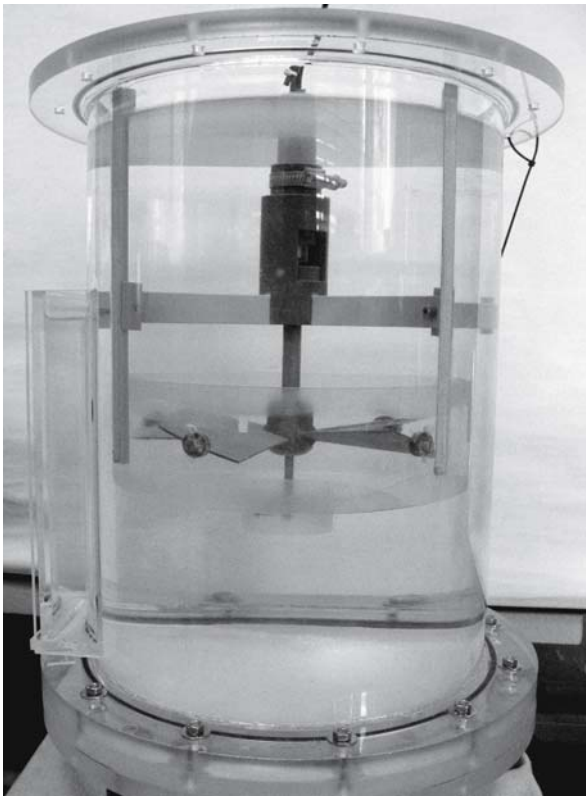

Fig. 3.6.
Benthic Water-Column-Simulator (BWCS) equipped with an optical window for LDA measurements (*left side*)

The newly developed Benthic-Water-Column-Simulator is a dual-propeller system with adjustable pitch and shaft length (Fig. 3.6). The propeller system itself is housed inside a cylinder (diameter $D = 290$ mm, overall height = 420 mm), with the first propeller plane at a height of 180 mm above the bed. The pitch angle α_p of this four-bladed propeller (diameter $D_{p1} = 200$ mm) is adjustable between +30 deg and –30 deg. The propeller blades terminate in a skirt of 70 mm height. The second propeller (diameter $D_{p2} = 50$ mm) is a fixed pitch ($\alpha_P = 40$ deg) three-bladed propeller. The propeller blades also terminate in a skirt (30 mm height). Both propellers are fixed on a single shaft and rotate at the same frequency. The distance of both propellers on the shaft relative to each other and the bottom of the BWCS is adjustable. Consequently, by adjusting the pitch of the uppermost propeller and changing the direction of rotation, four different operational modes can be realized – two propellers with opposite or same pitch and clockwise or counter clockwise rotation.

Due to the mainly rotational character of the BWCS flow there is a difference in comparison to the open channel flow of a river flow. In the BWCS the main flow component is the peripheral flow component u. In addition the mean radial flow component and the mean vertical flow component which are negligible in-situ are present in the BWCS. However, these components should be negligible compared to the peripheral flow component in general. The radial and vertical dependence of all velocity

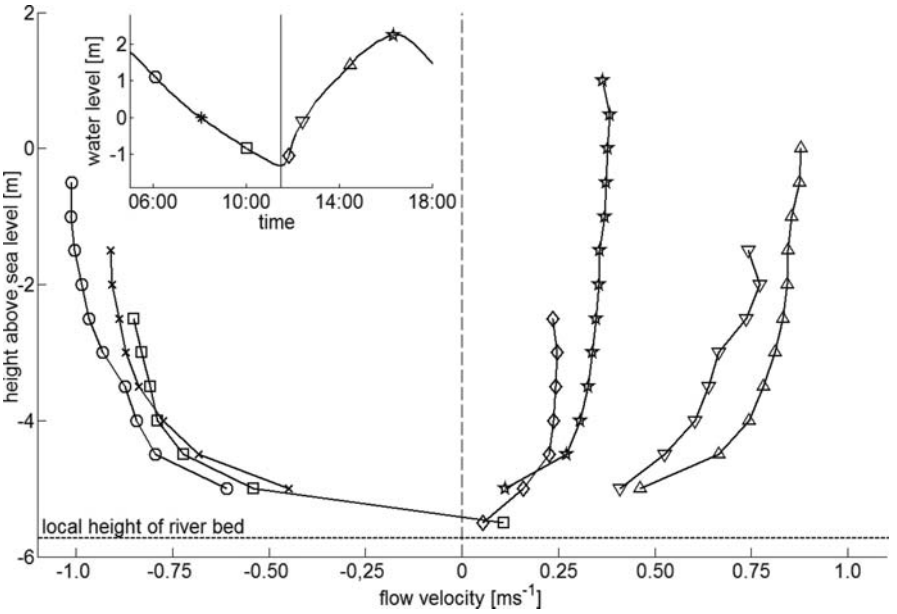

Fig. 3.7. Representative results showing flow velocity (m s^{-1}) against height (m) of the normal flow component through a cross-section at the river Elbe (Süderelbe, near Oortkaten, at September 25, 2003) obtained with a Broadband-ADCP during one tidal cycle

components also leads to anisotropy of turbulence and a radial distribution of bottom stress. Consequently, the design and especially the operational modes of the BWCS have to ensure, that these device-dependent differences will not influence the small scale processes to be investigated.

The design of the BWCS has to meet requirements arising from the variability of bottom stress and turbulence in natural flow. One regional focus of the SEDYMO project was the river Elbe, thus the BWCS need to fulfill the in-situ conditions of the tidal dominated estuary of this river at least. Synchronous measurements with a Broadband-ADCP system and a lowered Single-Point-ADV system were carried out during one tidal cycle to obtain characteristic in-situ data on flow turbulence and bottom shear stress. The mean flow characteristic (Fig. 3.7) was continuously monitored by the ADCP-system and the ADV-system recorded the depth-dependent 3-D turbulence characteristic (Fig. 3.8). Data were sampled at a frequency of 25 Hz. Using the ADV capability to measure the near-bottom distance with high precision, the bottom shear stress was determined by

$$\tau_b = \mu \lim_{z \to -h} \left(\frac{\partial u}{\partial z} \right) \quad , \quad u_* = \sqrt{\frac{\tau_b}{\rho}} \tag{3.2}$$

where μ = dynamic viscosity, u = depth-dependent mean flow velocity, h = depth, ρ = density and u_* = friction velocity. The origin of the coordinate system used is located at the (time-dependent) water surface with the vertical axis directed upward.

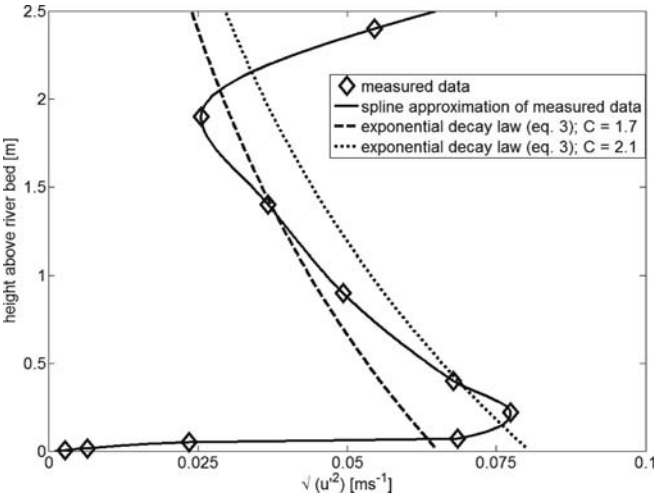

Fig. 3.8.
Representative results for depth-dependent flow turbulence obtained with a lowered Single-Point-ADV system (same location and time as data from Fig. 3.7)

The acquired field data from river Elbe established the range and upper values of turbulence intensities, mean flows and bottom stress for the design of the BWCS. In absence of the water–air boundary layer the field data on turbulence intensity fits the exponential decay law

$$\frac{u'}{u_*} = C\exp\left(-\frac{z+h}{h}\right), \quad C \cong 2.3 \tag{3.3}$$

as proposed by Nezu and Nakagawa (1993). We found that over a tidal cycle the value of the constant C varies in range between 1.7 and 2.1. For the design of the BWCS the value of $C = 2.3$ was taken as the upper limit for realistic turbulence intensities coupled to the friction velocity u_* as the main design parameter.

3.3.3 Characteristics of the Benthic Water-Column-Simulator

Compared with existing but more simple flow chambers and erosion devices, where only one parameter (e.g., frequency of the rotating disk) can be adjusted, the variety of adjustable parameters (frequency, pitch, distance of the both propeller and operational modus) leads to a large amount of calibration details. For calibration of the BWCS temperature-compensated hot film technique (Hensse et al. 1997) and a DANTEC 2-D LDA system were applied. The hot film technique provides the friction velocity (mean and fluctuation) and the LDA system was used to record velocity and turbulence of the flow at selected locations in the water column of the BWCS.

Results from first measurements confirmed the expectation that two optimal operational modes exist, one a so-called 'propeller mode' and the other a so-called 'microcosm mode'. The propeller mode is characterized by an orientation of pitch and direction of rotation such that both propeller generate a rotational flow which is directed towards the bottom of the BWCS. The principle of continuity leads to an upward di-

rected rotating flow within the gap between housing and skirt of the four-bladed propeller. The microcosm mode is characterized by an orientation of pitch and direction of rotation such that the four-bladed propeller (the upper one) operates in the same mode as at the propeller mode, but the three-bladed propeller (lower one) operates in the opposite rotation. A flow inside the BWCS similar to that inside the Gust microcosm (rotational flow with a central suction part and an outer region where the secondary flow is directed towards the bottom) is thus generated. A BWCS with a four-bladed propeller with a developed area ratio DAR = 1.0 and pitch $\alpha_p = 0$ deg produces a similar flow field to the Gust microcosm.

The experimental work to calibrate the flow inside the BWCS was supported by a flow simulation model using the Navier-Stokes-Equation-Solver COMET. Due to the sensitivity of the flow to small geometrical changes a validation of the numerical simulation method was executed by comparison of results from simulating the Gust microcosm with extensive LDA measurements of the overall flow. The results shows a good agreement except for the highly turbulent central region where either simulation or experimental data are discordant. The next level of flow simulation simulated a propeller inside a cylinder and we again compared the results with measured data. The established numerical flow model is suitable for design of single-propeller BWCS and similar flow chambers or erosion devices such as the EROMES system.

The simulation results are used on one hand to establish an effective grid of measuring points which allows a timesaving calibration procedure but on the other hand to guarantee that any overlooking of a flow sensitive region cannot occur. Flow sensitive regions are characterized by unstable flows which could appear at the central axis, the regions of strong flow interaction between the both propellers (esp. at the microcosm mode) and in the region with the radius $D_{p1}/2$ of the uppermost propeller.

Control Parameter: Bottom Shear Stress

To calibrate the BWCS for the control parameter bottom shear stress or friction velocity u_* this was measured by the hot film technique at radius $r = 0$, 54, 92, 110 and 130 mm. Data were sampled at a frequency of 25 Hz over 6 minutes to obtain a sufficient sample for statistical evaluation. For comparison of the results at different operational modes and/or changed geometric configuration an area-weighted value of friction velocity

$$u_* = \frac{1}{\left(\frac{D}{2}\right)^2} \sum_{i=1}^{N} \left[\left(\left(\frac{r_{i+1} + r_i}{2} \right)^2 - \left(\frac{r_i + r_{i-1}}{2} \right)^2 \right) u_{*_i} \right] \tag{3.4}$$

was calculated from the time-averaged values u_{*_i} at the radii r_i. The pitch α_p was set to $\alpha_p = 10$, 20 and 30 deg and the distance d between both propellers was set to $d = 155$, 130, 100 and 65 mm. The distance H of the uppermost propeller to the bottom always remained at $H = 180$ mm. The rpm-values ranged from 20 to 180 rev. min^{-1}. Measurements were performed under all four different operational modes but only results for the most different modes are presented here.

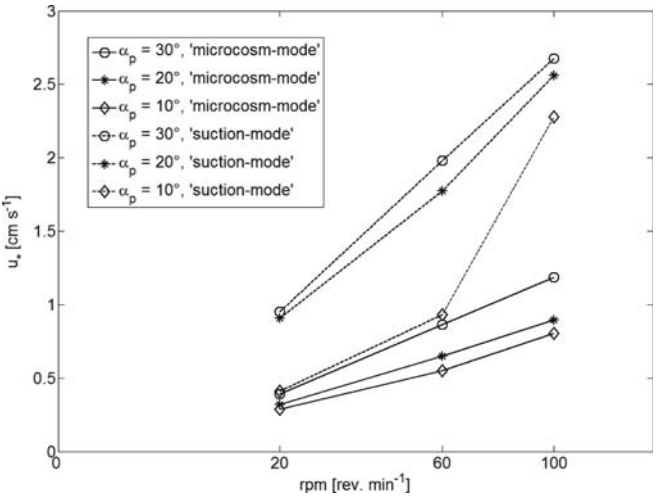

Fig. 3.9.
Characteristics of the BWCS for area-weighted friction velocity (cm s^{-1}) depending on operational mode, pitch angle of the uppermost propeller and revolutions per minute (rev. min^{-1})

The selection for the two operational modes (suction mode and microcosm mode) is on one hand due to the different flow stability these modes provide and on the other hand due to the very different hydrodynamic characteristics for each (see Fig. 3.9). In the microcosm mode and the propeller mode a very sensitive investigation of fine sediment dynamics at low friction velocities is possible. At the same rpm the area-weighted values of friction velocity generated in the BWCS are lower than at a comparable setting in the Gust-microcosm.

In the suction mode (area-weighted) bottom shear stress up to $\tau_b = 1$ N m^{-2} ($u_* \cong 3.2$ cm s^{-1}) were generated. Here an extension of the operational range of the Gust-microcosm is achieved and investigations on the erosion-deposition cycle of more erosion-resistant sediments can be performed. The influence of pitch angle changes can clearly be seen in Fig. 3.9. At the pitch angle $\alpha_p = 10$ deg the flow characteristics is more similar to the original Gust-microcosm, especially at low rpm. To generate stable flow conditions, especially at the suction mode, we recommend pitch angles $\alpha_p \geq 20$ deg.

Changing the distance between the propellers had only a weak influence on the area-weighted bottom shear stress. In the microcosm mode, which has the greatest sensitivity to this distance, the values of the area-averaged friction velocity at rpm = 180 rev. min^{-1} differ by 15% between the minimal and maximal distance. In agreement with the numerical model, the greatest friction velocities were measured for maximum distance. At rpm = 20 rev. min^{-1} no significant difference due to changed propeller distance d was measured.

Control Parameter: Flow Turbulence

The synonym 'flow turbulence' is here used for turbulent phenomena as caused by turbulent fluctuations of the bottom shear stress τ_b' (resp. u_*') and by turbulent fluctuations u' in the water column of the BWCS. This differentiation is required because of the two measuring principles used for calibration of the BWCS. With the used hot film skin friction probes, the measurement of bottom shear stress and fluctuations

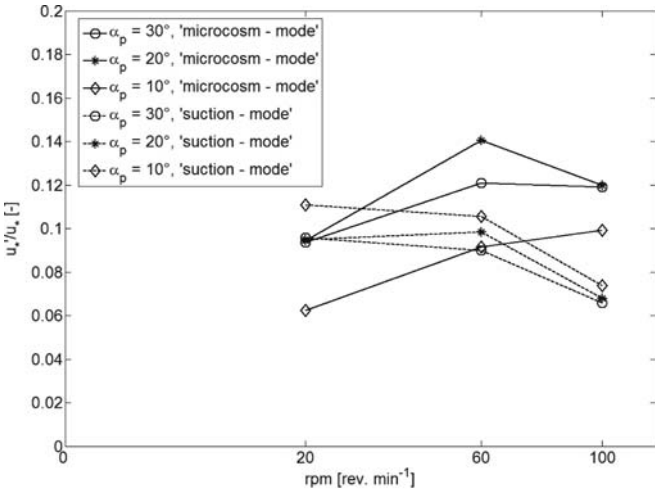

Fig. 3.10.
Characteristics of the BWCS for turbulence of friction velocity (ratio of fluctuations and mean; area-weighted values) depending on operational mode, pitch angle of the uppermost propeller and revolutions per minute (rev. min^{-1})

at the head of the BWCS are feasible, but not the measurement of the internal flow. With the LDA technique, the internal flow velocity and its fluctuations are measured. There is a connection between these measurements where a relationship similar to Eq. 3.3 exists for the very complex flow inside the BWCS.

From the hot film measurements the turbulent fluctuations of the bottom shear stress were obtained (Fig. 3.10). Both of the presented operational modes shows a slightly different behavior, yet, the values remain around $u_*'/u_* \sim 0.1$ over the full range of rpm. This parameter shows clearly an advantage of the BWCS design. This value lies at the same range achieved with the Gust microcosm and is similar to that of open-channel flow (Gust and Müller 1997). The high bottom shear stress fluctuations which were observed for the EROMES system (simple stirrer principle) (Müller et al. 1995) were effectively reduced but the advantage of a propeller system was maintained – reaching high values of friction velocity at moderate rpm. The characteristic feature of a Gust microcosm – rising friction velocity turbulence with growing rpm – as well as the constant or slightly decreasing turbulence of a propeller system with growing rpm were found in a less pronounced manner for the BWCS.

Execution of the LDA measurements was not simple. By using a 2-D LDA system a coincident measurement of the 3-D flow velocity vector at the desired measuring points inside the BWCS was not possible. The measurement of the 3-D velocity was executed by a twofold 2-D measurement under the fulfillment of matching conditions for the peripheral velocity. The measurements covered the water column from near bed up to 60 mm above the height of the uppermost propeller plane. The first result is that the mean radial and vertical velocities are mostly 10 percent lower than the local peripheral velocity, except for the gap between the skirt of the uppermost propeller and the housing of the BWCS. Here a significant rising vertical velocity was measured (up to 50 percent of the peripheral velocity), leading to a rapid transport of particles and solutes to the top of the BWCS. Downward transport will occur through the propeller plane.

The characteristic of flow turbulence in the water column up to 250 mm height above bottom of the BWCS is shown (Fig. 3.11). This depth-dependent distribution of

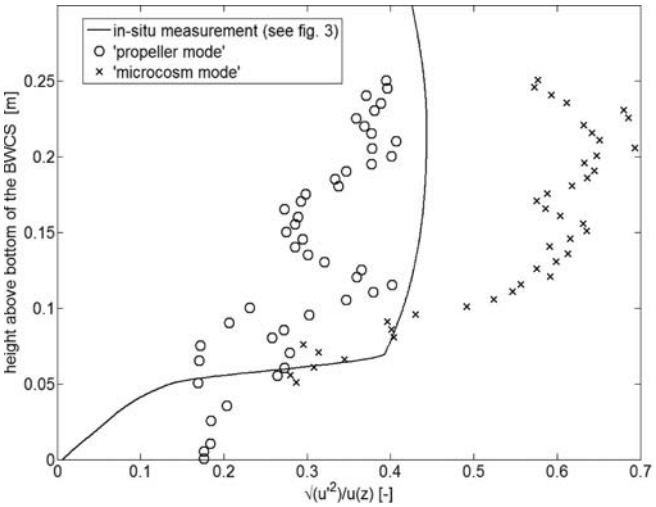

Fig. 3.11.
Representative results for flow turbulence against height (m) inside the BWCS depending on the operational mode compared to the in-situ measurement (see spline approximation of measured data at Fig. 3.8); the absolute value of the pitch of the upper propeller at both modes is $|\alpha_P| = 30$ deg

turbulence was measured at a radius of $r = 119$ mm. Vertical profiles at other radii look similar. The measured differences between microcosm mode and propeller mode as documented (Fig. 3.11) are caused by flow interaction of both propellers. Due to the opposite action of the two propellers in the microcosm mode the turbulence intensity is larger in this mode. More detailed tuning of the propeller design should allow an exact matching of an in-situ measured near-bed depth-dependence.

3.3.4 Conclusions

The newly developed *B*enthic-*W*ater-*C*olumn-*S*imulator (BWCS) is an effective tool for laboratory investigations of fine sediment dynamics. It merges the advantages both of the Gust-microcosm and the EROMES system. Synchronous reproduction of the small scale flow and bottom shear stress characteristics of natural flows similar to an open channel flow can be achieved segment-wise for the whole water column with the BWCS filled with artificial or natural sediments. At the present development stage, the system is calibrated up to bottom shear stress $\tau_b = 1$ N m^{-2}. The construction of the system is simple and robust. Within the SEDYMO project this device was applied for erosion and entrainment measurements. The reader is referred to the corresponding contributions (Kleeberg 2006; Paterson 2006; Siepmann 2006).

Acknowledgments

We would like to thank the Hamburg Port Authority and the Project Management Group at the Federal Ministry of Education and Research for a very successful cooperation. This work was funded by the Federal Ministry of Education and Research under contract no. 02WF0318.

References

Brunk B, Weber-Shirk M, Jensen A, Jirka G, Lion LW (1996) Modeling natural hydrodynamic systems with a differential-turbulence column. J Hydraulic Engineering 122(7):373–380

Gust G (1990) Method of generating precisely-defined wall shearing stresses. US Patent Number: 4,973,165,1990

Gust G, Müller V (1997) Interfacial hydrodynamics and entrainment functions of currently used erosion devices. In: Burt N, Parker R, Watts J (eds) Cohesive sediments – Proc. 4th nearshore and estuarine cohesive sediment transport conference INTERCOH '94, Wallingford 1994. Wiley, Chichester, UK:149–174

Hensse J, Müller V, Gust G (1997) Dynamic temperature compensation for hot film anemometry in turbulent flows – necessity and realisation. In: Shen X, Sun X (eds) Modern techniques and measurements in fluid flows – Proceedings of the 3rd conference on fluid dynamic measurement and its applications, Beijing 1997, Int. Academic Publishers, Beijing, P.R. of China, ISBN 7-80003-407-0/TB

Kleeberg A, Hupfer M, Gust G (2007) Phosphorus Entrainment due to Resuspension, river Spree, NE Germany. This volume

Müller V, Vorrath D, Werner A, Witte G (1995) Schubspannungscharakteristik des EROMES-Systems – Messungen zur Hydrodynamik und Erosionsversuche mit Kaolinit. report GKSS 95/E/43, Geesthacht, Germany, ISSN 0344–9629

Nezu I, Nakagawa H (1993) Turbulence in open-channel flow. IAHR Monograph Series, A. A. Balkema Publishers, Rotterdam, Netherlands

Paterson D (2007) On the Boundaries: Measurements of Extreme Systems. This volume

Siepmann R, von der Kammer F, Calmano W (2007) Mobility of Heavy Metals from Resuspended Anoxic Sediments – Close to Nature Approach in Benthic Chambers. This volume

Tengberg A, Stahl H, Gust G, Müller V, Arning U, Andersson H, Hall POJ (2004) Intercalibration of benthic flux chambers I. Accuracy of flux measurements and influence of chamber hydrodynamics. Progress in Oceanography 60:1–28

Gregor Kühn · Gerhard H. Jirka

3.4 Fine Sediment Behavior in Open Channel Turbulence: an Experimental Study

3.4.1 Introduction

Water quality in natural rivers is strongly related to the occurrence of fine sediment particles in the water body. Fine sediment particles offer large surface areas relative to their volume and a high adsorption potential leading to electrostatic agglomeration of contaminants at the particle surface. Furthermore, chemical reactions that occur at the particle surface modify the contaminants. To study contaminant transport in rivers the behavior of fine particles under natural conditions has to be investigated. The important processes are aggregation and disaggregation, leading to floc sizes of different orders of magnitude.

The driving mechanical force in the system is induced by the flow. The flow velocity is composed of a mean flow and the turbulent velocity fluctuations around the mean. The velocity fluctuations are responsible for shear forces and collision of single particles (van Leussen 1994). Therefore, the transformation of the floc size is strongly related to the turbulence conditions in the open channel water column as described by Nezu and Nakagawa (1993).

In an improvement of the differential turbulence column (Brunk et al. 1996) the turbulence is well-controlled and the particle size and the concentration profile can be observed in order to obtain a relationship between mass concentration and shear forces affecting aggregation and disaggregation. This system was used to simulate these processes for different conditions like in nature.

3.4.2 Experimental System

The system was designed to simulate the turbulence profile of open-channel flow using grids oscillating at different frequencies distributed over the vertical column. Thus, the particle behavior over time can be studied locally under-well-controlled turbulence without advection taking place. In open-channel flow particles are advected with the mean flow and therefore, not traceable with stationary measurement equipment on their path in the river though changing environmental conditions. Based on the studies of Brunk et al. (1996) a differential turbulence column was constructed to reproduce a turbulence profile typical for open channel flows, such as rivers (Nezu and Nakagawa 1993).

Sridic et al. (1996) showed the advantage of using oscillating grid pairs instead of single grids to produce a larger area of homogeneous turbulence and amplifying the turbulent fluctuations additionally. In the present study, five pairs of oscillating grids

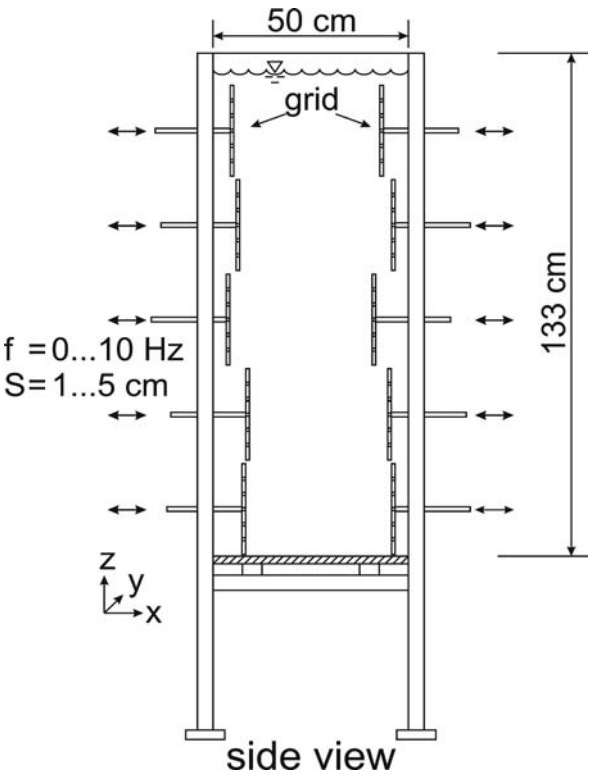

Fig. 3.12.
Sketch of the differential turbulence column

were arranged vertically in a perspex tank (Fig. 3.12). The plan dimensions were 50 × 35 cm, while the height was 133 cm. Each grid was controlled separately via PC and could be adjusted to different frequency and strokes, leading to turbulence characteristics as given by Hopfinger and Toly (1976).

To determine the flow characteristics in the tank different methods for velocity measurement were used. A Laser Doppler Velocimeter (TSI Corp.) was adapted to an automatic traversing system to measure the mean flow and the turbulence intensities in vertical profiles. To get an impression of the complete flow field in the middle region of the tank Particle Image Velocimetry (PIV) was used. Therefore an PIV-System (LaVision) with an 20 mJ Nd:YAG Laser and a CCD camera was installed.

To investigate changes in the particle size distribution of the suspended sediment particles under given turbulence conditions, an in-line microscope (Aello 7000) was used. The microscope consists of an stainless steel tube with a diameter of 38 mm which has a 8 mm wide gap in the mid-section, where the CCD sensor of a fire wire camera and illumination unit are located. The camera can resolve particles between 4 and 500 µm which are located in the focal plane behind the sapphire observation window. The in-line microscope could be inserted into the differential turbulence column at different positions through process inlets, while the system was running. Seven of these inlets were located on the back of the tank at different levels. The images were analyzed with image recognition software to detect particles and to determine their size in the focal plane. For that purpose a two-step analysis was used. In the first step, sharp edges were detected. In the second step contiguous areas were analyzed. Regions with contiguous area and sharp edges are counted as particles.

The measurements of the particle size were completed by measuring the water column turbidity continuously to record the mass distribution of sediment. A single turbidity sensor (Honeywell APMS-10GRCF-KIT) with a automatic sampling unit was positioned at seven sample positions with height over the chamber. The sample positions were measured concurrently. At the end of each cycle a reference fluid was measured and between each change of position the sensor was flushed. This cycle was continued for the complete time of an experiment. The sensor was also individually calibrated to each type of sediment.

3.4.3 Results

Turbulent Flow Field

A key precondition for conducting experiments on floc size distribution is a well controlled turbulence distribution in the tank. For the first phase it was necessary to determine the turbulent conditions in the differential turbulence column and optimize it to represent the profile of the turbulent intensities of an open channel flow. For these measurements the LDV was used, with a measurement location in the center of the column. The agitation conditions of the oscillating grids were based on the result of Brunk et al. (1996). The frequencies of the grids were varied between 1 Hz to 6 Hz. The stroke was varied between 2 cm and 5 cm. Finally the stroke was fixed at 3 cm to span a wide range of useful turbulent fluctuations.

PIV measurements at 14 different positions were taken (Fig. 3.13). The bottom grid frequency was set to 4 Hz. The mean flow shows clear secondary flow cells with flow velocities less than 5 cm s^{-1}. This flow is result of the geometry and production of turbulence by the oscillating grids. The size of these cells correspond with the size of the grids.

The turbulence intensity can be expressed as turbulent kinetic energy $k^{1/2}$, defined as

$$k = \mathrm{TKE} = \frac{1}{2}\left(u'^2 + v'^2 + w'^2\right) \tag{3.5}$$

in which u', v' and w' are the velocity fluctuations in x-, y- and z-direction (Fig. 3.13b).

With the assumption of isotropy, the turbulent kinetic energy can be written as

$$\sqrt{k} = \sqrt{\frac{3}{4}\left(u'^2 + w'^2\right)} \tag{3.6}$$

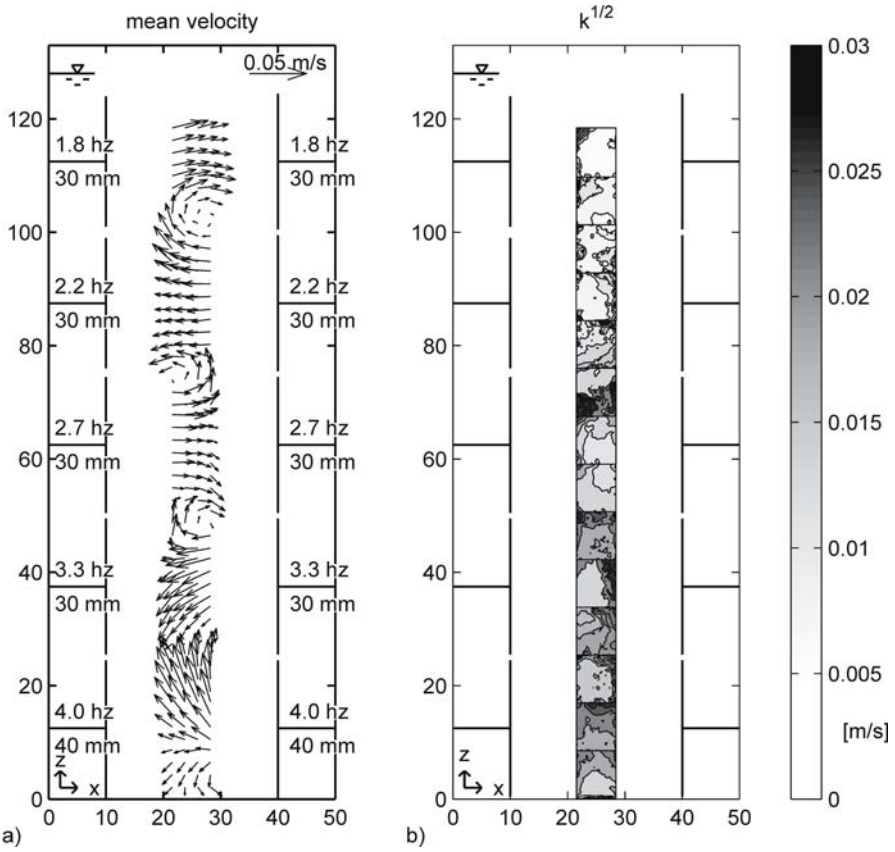

Fig. 3.13. a Mean velocity and **b** turbulent kinetic energy in the center region of the differential turbulence column, measured by PIV

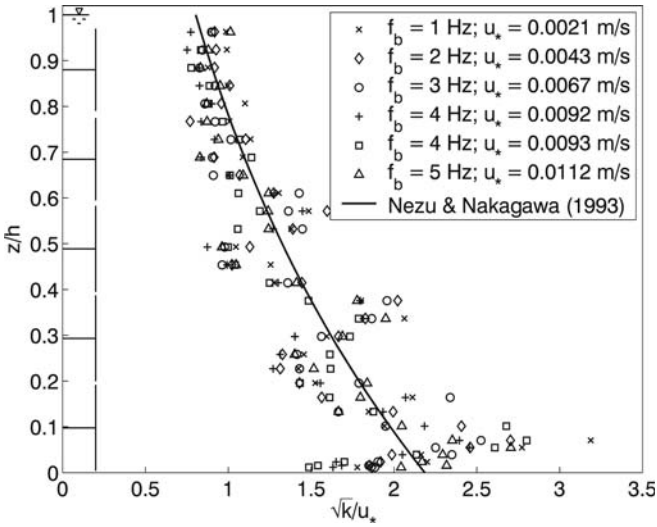

Fig. 3.14.
Distribution of the turbulent kinetic energy for different turbulent conditions

The distribution of k in the center region is given (Fig. 3.13). The turbulent kinetic energy decreased towards the surface, while in the center region it stays laterally constant. Close to the bottom the fluctuations were damped to zero. The turbulent fluctuations represented by the RMS-velocities were slightly stronger than the secondary flow.

The LDV measurements were obtained to visualize the distribution of the turbulent fluctuations (Fig. 3.14). The result of different agitation conditions from 1 Hz to 5 Hz of the bottom grid frequencies, scaled by the water depth and a corresponding shear velocity $u_\star$ were recorded (Fig. 3.14). In comparison the vertical profile of the turbulence intensities in a natural river as determined by Nezu and Nakagawa (1993) was also plotted. In detail, the effect of the oscillating grids was seen in the distribution of the turbulence intensities. Due to the different frequencies of the grids and their resultant movement in opposite directions, an increase in turbulent fluctuations at the gap between two pairs of grids was observed. This produces strong peaks of turbulent intensities between pairs of grids. In the center of a pair of grids the production of turbulence is decreased because of the lesser fringe effects. However, the average of turbulent fluctuations in the differential turbulence column fell within the natural range of conditions of an natural river.

Particle Size Distribution and Development

The second phase of work was to determine the behavior of fine sediment under turbulent conditions. In the present case kaoline (Dorfner H III GF) was used to represent the sediment and to remove the influence of the complex mixture of different ingredients in natural sediment. Kaoline is one of the largest fractions in natural fine sediments. The sediment concentration was in a range from 100 to 1 000 mg l^{-1} under different turbulent conditions. At the beginning of the experiment, the sediment was completely mixed into the water column. During the experiment, the particle size distribution was measured at a constant height with the Aello microscope. After a steady state

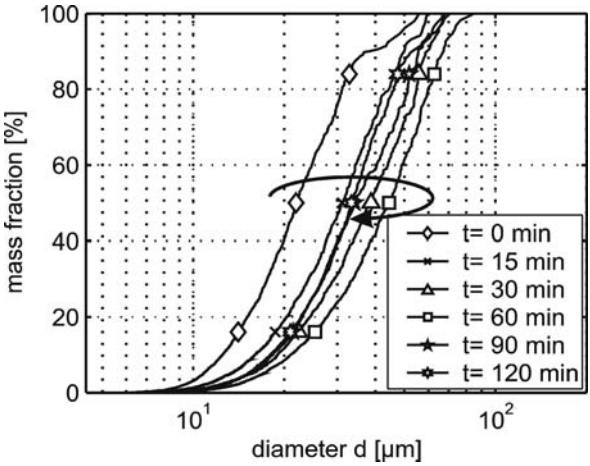

Fig. 3.15.
Evolution of the particle size of kaoline at $z/h = 0.68$ with a mean concentration of 500 mg l^{-1}

of the particle size distribution was reached, the microscope was used to measure the sediment size distribution at seven different heights. Simultaneously, the turbidity was measured at the same seven positions during the complete experiment.

The evolution of the volumetric particle size distribution over time was recorded (Fig. 3.15). The initial concentration of kaoline was 500 mg l^{-1}. The frequency of the bottom grid was 1 Hz. The measuring plane of the microscope was positioned in the center of the column at $z/h = 0.68$.

While the experiment was running an increase of the particle size could be observed from $t = 0$ min to $t = 60$ min. After reaching a maximum particle size at $t = 60$ min, the particle size decreased reaching a steady state after approximately 90 min. This phenomenon can be explained by the development of a mass concentration profile, starting from fully mixed conditions. This will be shown later using the turbidity measurements. The particle size in the steady state is larger than the initial particle size, which means that under the given turbulence conditions particle aggregation is taking place.

After achieving the steady state particle size distribution, the position of the microscope was changed over height, so that a volumetric size distribution profile could be measured (Fig. 3.16).

The particle size increased towards the surface in accordance with decreasing turbulence. In the upper region, the turbulence and therefore, the shear forces are small enough to allow aggregation. The largest particle size distribution was found at the second level at $z/h = 0.68$. This can be explained using the mass concentration profile (Fig. 3.18). In the top level the amount of sediment material is so small, that the random conjunction of two particles is relatively rare and the fabric of the aggregated particles is not very strong. The effect of doubling the turbulence intensities on particle size distribution was investigated (Fig. 3.17). The initial particle size distribution was the steady state of the described experiment. The particle size distribution was measured as before at $z/h = 0.68$ in the center of the column and the volumetric particle size distribution at different time steps was recorded (Fig. 3.17). At time $t = 0$ min the particle distribution shows larger particles due to aggregation that occurred under

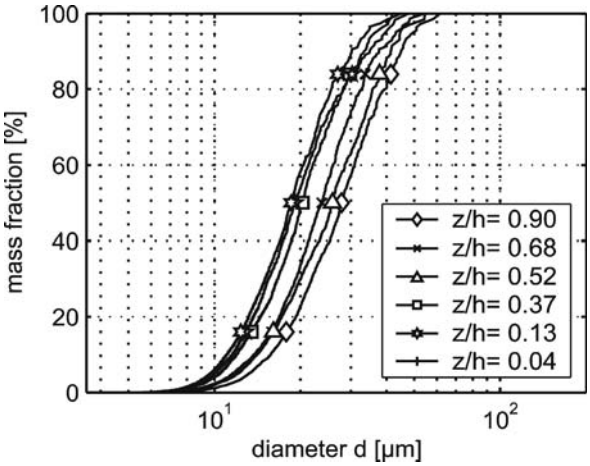

Fig. 3.16.
Distribution of floc size of kaoline over depth at $t = 240$ min with a mean concentration of 500 mg l^{-1}

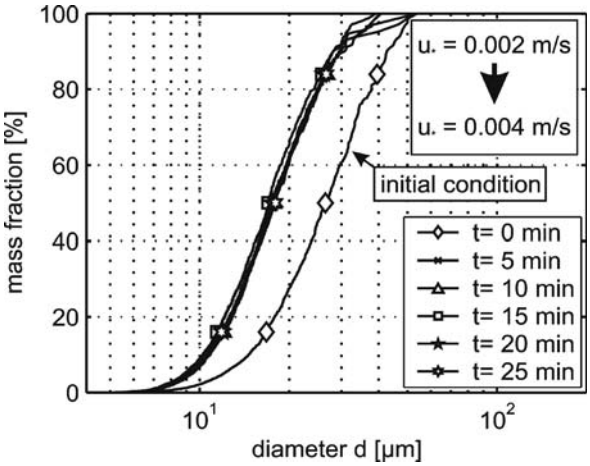

Fig. 3.17.
Segregation of kaoline flocs with a mean concentration of 500 mg l^{-1} by doubling the turbulent intensity at $z/h = 0.68$

the previous low turbulence regime. After $t = 5$ min with the turbulent intensity doubled, most of the aggregates were destroyed and the distribution again reached a steady state, with smaller particle sizes similar to the initial conditions at the beginning.

Additional to the investigation of particle size, the mass concentration in the differential turbulence column was also measured with a turbidity sensor at the same heights. Scaled by a calibration, the data can be transformed into mass concentration profiles. The artificial sediment Kaolin was used with an initial concentration of $c_0 = 500$ mg l^{-1}, fully mixed into the differential turbulence column. The calibrated mass concentration at different levels for different turbulent conditions was recorded (Fig. 3.18). Initially, the turbidity in the top region started to decrease after 20 min followed by a decrease in turbidity at lower levels. This diagram represents pure particle settling (Fig. 3.18a). In the next case (Fig. 3.18b) the bottom grid frequency was 1 Hz, with lower frequencies in the upper layers to simulate an open channel turbulence profile. A slight settling tendency in the complete water body was noted. However, in the two upper regions an

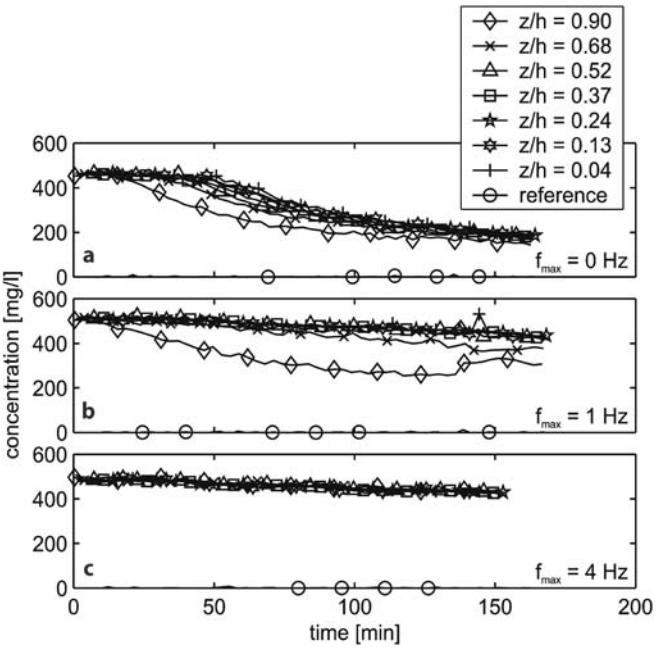

Fig. 3.18.
Mass distribution evolution of kaoline at various turbulent conditions, **a** no agitation and pure settling, **b** low turbulence with 1 Hz bottom grid frequency, **c** stronger turbulence with 4 Hz bottom grid frequency

additional decrease of mass was observed at the beginning. The timescale for developing the mass stratification is about $t = 90$ min, the same as for reaching a steady state of the particle size distribution. In the lower region the suspension remains fully mixed with homogeneous concentration due to the higher turbulence level.

In the last case shown, the turbulence of the bottom grid frequency was increased to 4 Hz. In this case only a slight sedimentation was observed. The suspension in the water body remained fully mixed and the mass distribution over depth is constant (Fig. 3.18c).

3.4.4 Conclusion and Outlook

For investigating the behavior of fine sediment particles under turbulence conditions similar to open channel flow a differential turbulence column was designed. Oscillating pairs of grids were used to produce a turbulence profile. Velocity measurements using LDA and PIV demonstrate that the turbulence conditions in the column can be well controlled. The turbulence profile can be adjusted to represents average conditions of open channel river flow. Secondary flow in the column due to the geometry and the agitation has been suppressed as much as possible so that its influence on the particles can be neglected.

The evolution of the particle size of the particle ensemble and of the concentration profile was observed by an in-situ microscope and by continuously sampling the turbidity at 7 different levels. The investigation showed a tendency for single particles to build aggregates in regions of low turbulence. The size of the aggregates was limited by the shear forces due to the turbulent conditions and the amount of mass.

The investigations on the particle size distribution and the concentration profile will be used for calibrating a numerical model (Ditschke and Markofsky 2006). For that purpose additional experiments are planned with other artificial and natural sediments, including those containing biological activity.

Acknowledgments

This research is supported by the German Federal Ministry of Education and Research in the framework of the joint project Sedymo (Fö-Nr: 02WF0317).

References

Brunk B, Weber-Shirk M, Jensen A, Jirka G, Lion L W (1996) Modeling natural hydrodynamic systems with a differential-turbulence column. J Hydr Eng 122:373–380

Brunk B (1997) Turbulent Coagulation of Particles Smaller Than the length Scales of Turbulence and equilibrium Sorption of Phenantrene to Clay. Ph.D. Thesis, Cornell University, New York

Ditschke D, Markofsky M (2006) A non-equilibrium, multi-class flocculation model. Proc. SEDYMO International Symposium 2006, Hamburg

Fengler G, Köster M, Meyer-Reil L-A (2006) Sediment erodibility in an intertidal groyne field of the Elbe River: Impact on microbial mediated processes. Proc. SEDYMO International Symposium, Hamburg

Hopfinger EJ, Toly JA (1976) Spatially decaying turbulence and its relation to mixing across density interfaces. J Fluid Mech 78:155–175

Nezu I, Nakagawa H (1993) Turbulence in Open-Channel Flow. Rotterdam, Brookfield: A. A. Balkema

Srdic A, Fernando HJS, Montenegro L (1996) Generation of nearly isotropic turbulence using two oscillating grids. Exp Fluids 20:395–397

Van Leussen W (1994) Esturaine Macreoflocs and their Role in Fine-Grained Sediment Transport. Ph.D. Thesis, University of Utrecht, Utrecht

Marion Köster · Lutz-Arend Meyer-Reil · Günter Fengler

3.5 Influence of Microbial Colonization on the Sediment Erodibility in an Intertidal Groyne Field of the River Elbe

3.5.1 Ecological Relevance of Erosion and Resuspension

The accumulation of fine grained cohesive sediments and their enhanced concentrations of inorganic and organic nutrients as well as pollutants is a wide spread problem in aquatic environments. For the estimation of the eutrophication risk of an aquatic ecosystem, detailed knowledge of the mobilization of polluted sediments by erosion is required for water resource management (Westrich and Förstner 2005). Erosion may be caused by natural events, such as water movement and biological activities, as well as anthropogenic impacts, such as dredging. During the last decades, the erosion of cohesive sediments and the resulting resuspension of particles in the water column have been identified as processes of high ecological relevance. This applies to the remobilization of nutrients required for pelagic primary production causing potential eutrophication as well as to the liberation of pollutants.

The erosion and subsequent resuspension of sediment particles is controlled by the current dynamics and the sediment stability. Benthic organisms which colonize benthic habitats have a great impact on sediment stability (Graf and Rosenberg 1997; Widdows et al. 2000, 2006). Among the biological effects, the secretion of extracellular polymeric substances (EPS) by (micro)organisms (e.g., de Brouwer et al. 2000, 2005) and bioturbation by meio- and macrofauna (e.g., Widdows et al. 2000; Roast et al. 2004) seem to be most important mechanisms of sediment stabilization and destabilization, respectively. Resuspension of sediments leads to the liberation of organisms (Shimeta et al. 2004) and particles as well as inorganic and organic matter into the water column. The suspended particles are modified and degraded through microbial activities thus causing the liberation of nutrients and pollutants. Since suspended matter can be transported over long distances, erosion and resuspension events may influence regions remote from the origin of the events.

The goal of this study was to investigate the influence of microbial communities on the sediment stability in an intertidal groyne field of the river Elbe (stream km 607.5). It was of special interest to investigate the sediment stability in relation to the composition and microbial colonization of resuspended sediments, and the prevailing hydrodynamic conditions.

Experimental Approach

Sediments were collected with a manually operated corer from the groyne field of the tidal Elbe during the sampling period from June 2003 to September 2005. Undisturbed sediment columns (inner diameter of 10 cm, length of 40 cm) were exposed to increasing shear stress in a particulate entrainment simulator (PES, Tsai and Lick 1986) comprising the range of shear stress expected in the field (>0 to 0.23 N m^{-2}). After 2 min exposure intervals, eroded sediment particles were taken with a 50 ml syringe from the overlying water and filtered on Whatman GF/C filters (for details see Fengler et al. 2006).

Sediment-specific erosion curves were obtained by plotting resuspended sediments (total particulate matter, TPM) versus shear stress. The critical erosion shear stress τ_{crit} was derived from erosion curves based on log transformed TPM data. The value τ_{crit} was defined as the threshold value above which the initial motion of sediment particles occurred (for discussions of the different approaches for the determination of the critical shear stress compare for example Grant and Gust 1987; Paterson et al. 1999).

The structure and chemical composition of eroded particles was described by their size spectra, contents of organic carbon and nitrogen (Köster et al. 1997), and trace metal contents (Petersen et al. 1996). For the (micro)biological characterization of the eroded particles, defined subsamples of suspended sediments were analyzed for total bacteria (Meyer-Reil 1983), photoautotrophic cells, total and photoautotrophic microbial biomass (Findlay et al. 1989; HELCOM 1988), and EPS (de Brower and Stal 2001). Enzymatic microbial degradation activity and fluxes of oxygen, ammonia, and phosphate were analyzed in time-course experiments according to Köster et al. (1997) and Meyercordt and Meyer-Reil (1999). Additionally, roller tank experiments (Shanks and Edmondson 1989; Ziervogel 2003) were performed to study properties of eroded sediment particles during transport processes (for details see Fengler et al. 2006).

3.5.2 Sediment Specific Erosion Curves and Critical Erosion Shear Stress

With increasing stabilization of the sediments, the slope of the sediment-specific erosion curves decreased (Fig. 3.19). The stability of sediments from the intertidal groyne field of the river Elbe varied spatially and seasonally with values for the critical shear stress between >0 and 0.07 N m^{-2}. Exposed sandy mud sediments at the edges of the groyne field showed higher stability as compared to the more muddy sediments in the center of the groyne field, which are less influenced by the currents. The stability of the sediments seemed to increase in summer and to decrease in autumn and winter during the investigation period from 2003 to 2005.

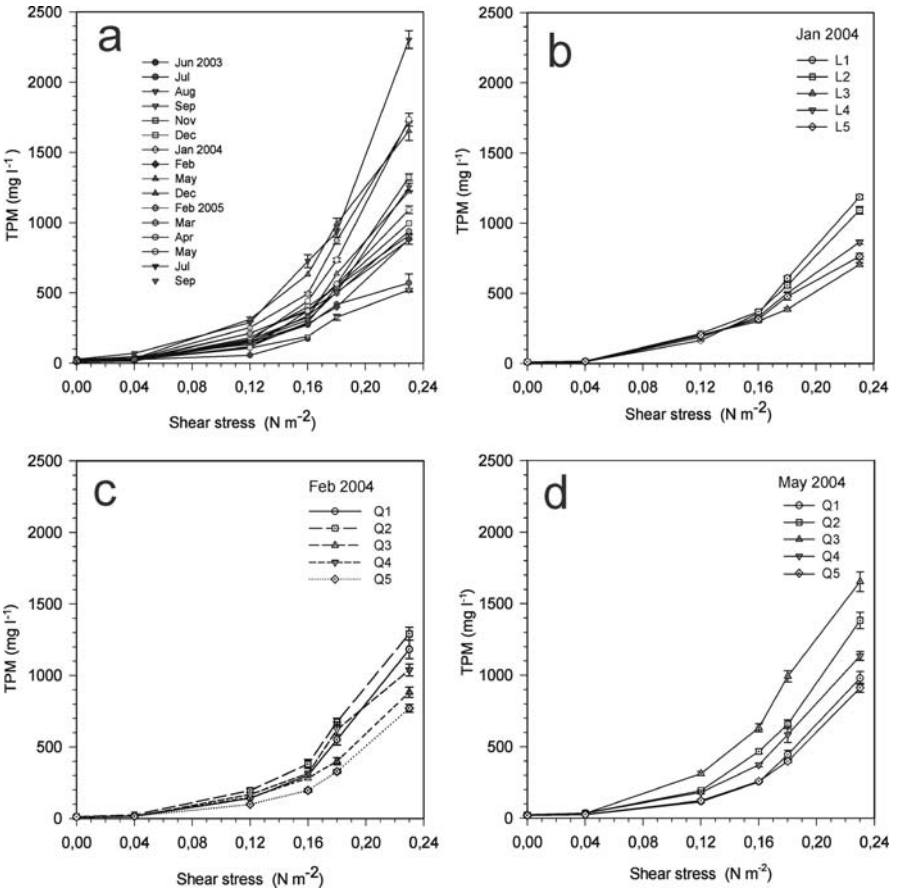

Fig. 3.19. Sediment-specific erosion curves obtained from sediments sampled at different sites in the groyne field of the river Elbe (**a** central station Z during the investigation period 2003–2005, **b–d** stations of the transects L and Q in January, February, and May 2004, respectively; *TPM:* total particulate matter). Error bars represent standard deviation ($n = 3$)

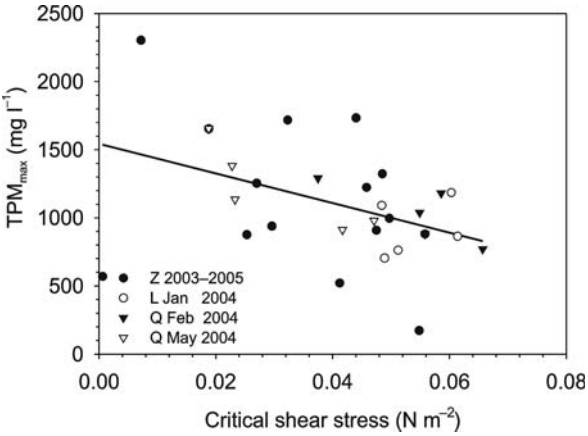

Fig. 3.20.
Relationship between maximum concentration of eroded particles (*TPM:* total particulate matter) and critical shear stress in sediments sampled at different sites in the groyne field of the river Elbe ($f(x) = -10\,865x + 1\,543$, $r = 0.427$; *Z:* central station during the investigation period 2003–2005; *L, Q:* stations of the transects *L* and *Q* sampled in January, February, and May 2004, respectively). The straight line indicates the linear regression curve

Critical shear stress of the sediments that was limited to the maximum applied stress in the system correlated significantly and inversely with the maximum concentration of eroded sediment particles. The higher the critical shear stress, the lower the number of eroded particles (Fig. 3.20). This significant relation underlines the validity of the determination of the critical shear stress derived from the sediment-specific erosion curves by extrapolation to the threshold value of particle liberation. A comparable relation between shear stress and liberation of particles was described by Widdows et al. (1998) for intertidal sediments.

Observations of the erosion process in the particle entrainment simulator showed that above the critical shear stress, small particles were randomly liberated from the sediment. The particles moved randomly on the sediment surface or were suspended in the overlying water. With increasing shear stress, larger particles and aggregates were released from the sediment (Fig. 3.21). The erosion was a highly dynamic process: smaller particles stuck together, and larger aggregates broke into smaller units. Beside erosion, deposition of aggregates on the sediment surface occurred. A layer of fluffy material on the sediment surface ("Sedimentauflage", Meyer-Reil 2006) was easily resuspended even at low shear stress.

3.5.3 Sediment Stability, Composition and Microbial Colonization of Resuspended Particles

The stability of sediments of the river Elbe was reflected in the number and size composition of resuspended particles. A high number of small particles (<30 µm) was released from sediments that were easily eroded. A comparable dominance of small particles was observed by Ploug et al. (2002) in the highly dynamic upper Elbe Estuary. Investigations with resuspended coastal sediments of the southern Baltic Sea showed that fine particles are main contributors to nutrient load (carbon, nitrogen) and sites of enhanced microbial colonization and activity (Rieling 2000).

The erosion experiments revealed that with increasing sediment stability, the number of particles released decreased. Their size spectrum was shifted to larger

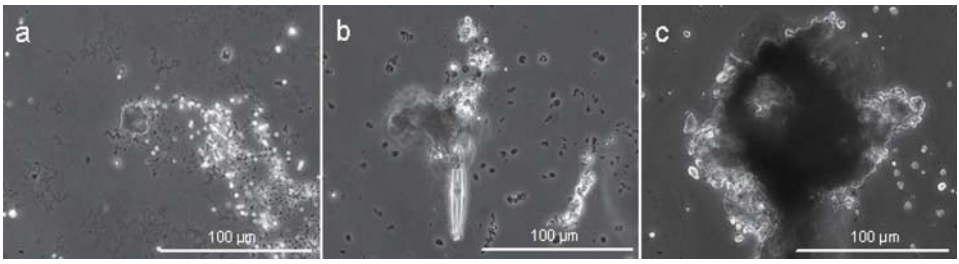

Fig. 3.21. Phase contrast micrographs of sediment particles eroded at different shear stress (**a** 0.50 N m^{-2}; **b** 1.00 N m^{-2}; **c** 1.25 N m^{-2}) from sediments of the river Neckar

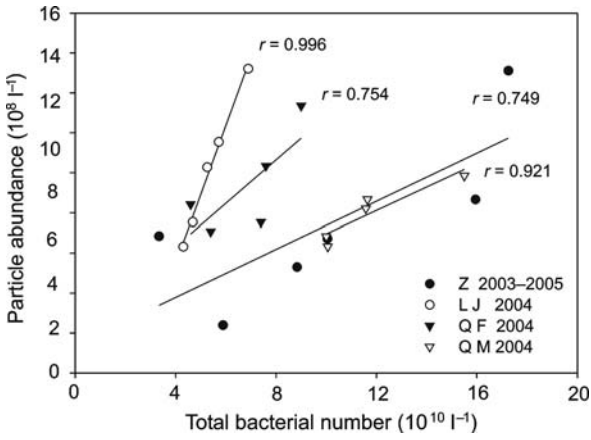

Fig. 3.22. Relationships between particle abundance and total bacterial number of eroded particles in sediments investigated at different sites in the groyne field of the river Elbe (*Z:* central station during the investigation period 2003–2005; *L, Q:* stations of the transects *L* and *Q* sampled in January, February, and May 2004, respectively). The *straight lines* indicate the linear regression curves

particles and aggregates. This applied especially to the exposed sandy mud sediments at the edges of the groyne field of the river Elbe. Sutherland et al. (1998) discussed that with increasing stability (time of non-disturbance) of the sediments, the size of the eroded particles increased. Resuspended particles from the groyne field of the river Elbe were intensively colonized by bacteria. The number of particles released was significantly correlated with the number of bacteria, although the relationship patterns differed depending upon season and location in the groyne field (Fig. 3.22). This may be explained by differences in the chemical composition of the particles and their colonization by different physiological and taxonomic groups of microorganisms.

Roller table experiments showed that the composition, microbial colonization and activity of resuspended particles altered during transport processes (Fengler et al. 2006). The particle size spectrum shifted from smaller (0–30 µm) to larger particles (31–150 µm) during a 7-d period. The ratio of organic carbon to nitrogen increased due to intense microbial metabolism in the dark. In the light the ratio decreased due to the formation of fresh organic matter by primary production as indicated by the increase of chlorophyll *a*. Pronounced increases in bacterial numbers, enzymatic microbial activity, and EPS were found within the first 2 d during light incubation.

3.5.4 Sediment Stabilization and Extracellular Polymeric Substances

Microorganisms (microalgae, bacteria, cyanobacteria) secrete extracellular polymeric substances (EPS), which consist of carbohydrates, proteins and a variety of other organic compounds (e.g., Decho 1990; Nichols et al. 2005). Because of their gel structure (Decho et al. 2003) and their high adsorption capacity, the EPS fulfill key functions for the organisms and in their environment (Köster and Meyer-Reil 2002). Beside their role in motility and adhesion of organisms to surfaces, EPS are important for binding organic and inorganic matter and pollutants, concentrating extracellular enzymes and supporting genetic transfer throughout the EPS matrix among the organisms (Decho 1990; Flemming and Wingender 2001). By the mediation of the properties of EPS, sediment particles are glued together. Because of their variable and complex chemical composition and function, the analysis of EPS and their relation to different functions is still a problem.

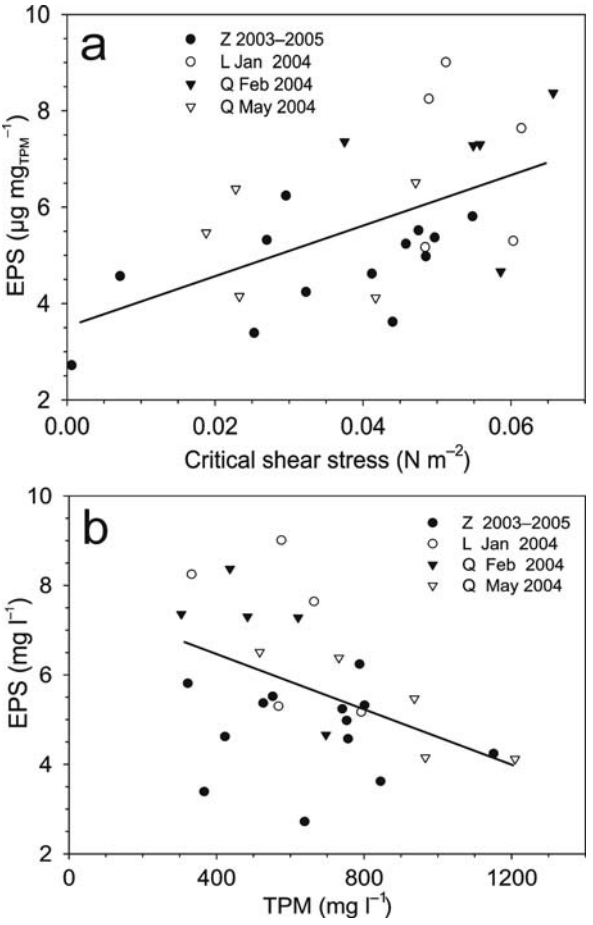

Fig. 3.23. Relationships between content of extracellular polymeric substances (*EPS*) of eroded particles and critical shear stress ($f(x) = 50.3x + 3.6$, $r = 0.537$) (**a**), and between EPS concentration and dry weight of resuspended particles (*TPM:* total particulate matter; $f(x) = 0.003x + 7.74$, $r = 0.458$) (**b**) in sediments investigated at different sites in the groyne field of the river Elbe (*Z:* central station during the investigation period 2003–2005; *L, Q:* stations of the transects *L* and *Q* sampled in January, February, and May 2004, respectively). The *straight lines* indicate the linear regression curves

The critical shear stress and the EPS content of the sediments were significantly correlated; the higher the EPS content, the higher the sediment stability (Fig. 3.23a). This relation was supported by the significant inverse correlation between the EPS concentration and the concentration of the resuspended sediments (TPM; Fig. 3.23b). From these observations it was concluded that increasing EPS contents enhanced the critical shear stress and therefore decreased the erosion risk in sediments of the groyne field of the river Elbe.

The source of EPS production in the sediments still remains unclear. Benthic microalgae, which are known to be the main EPS producers in shallow aquatic sediments (e.g., de Brouwer et al. 2005), can be discounted because of the low light intensity (2–3 μE m^{-2} s^{-1}). According to Ploug et al. (2002), light intensities of >7 μE m^{-2} s^{-1} are necessary to support positive photosynthesis. It could be proposed that planktonic microalgae deposited in the groyne field contribute to the EPS content of the sediments. This is supported by the significant correlation between contents of chlorophyll a and EPS (colloidal fraction, Fig. 3.24a). Whereas meio- and macrofaua can destabilize sediments through their movement, they may also contribute to the stabilization of

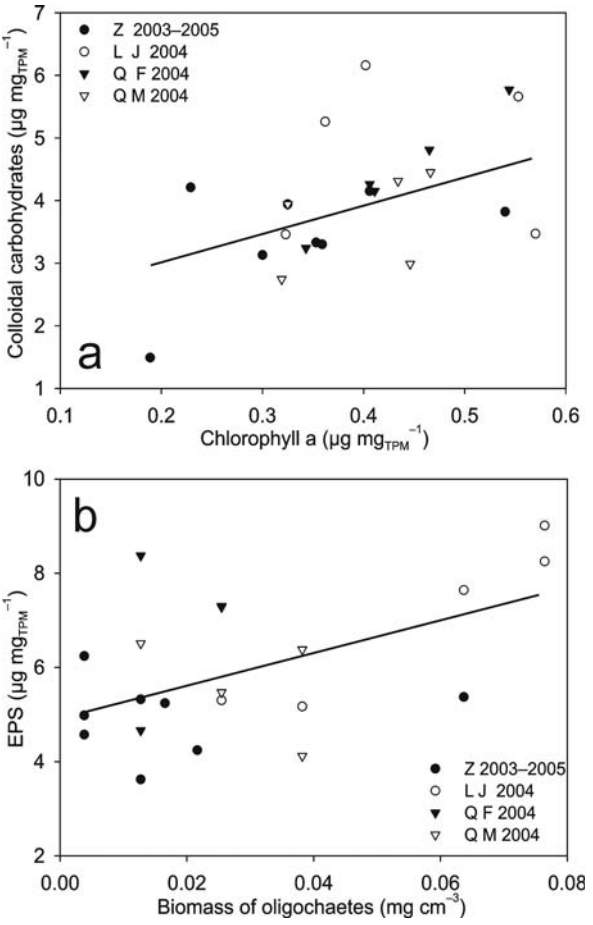

Fig. 3.24. Relationships between content of chlorophyll a and content of extracellular polymeric substances (EPS) ($(f(x) = 4.6x + 2.1$, $r = 0.457$) of eroded particles (**a**), and between EPS content and biomass of oligochaetes (expressed as mg wet weight per one cm^3 of sediment) ($(f(x) = 33.9x + 5.0$, $r = 0.515$) (**b**) in sediments sampled at different sites in the groyne field of the river Elbe (*Z:* central station during the investigation period 2003–2005; *L, Q:* stations of the transects *L* and *Q* sampled in January, February, and May 2004, respectively). The *straight lines* indicate the linear regression curves

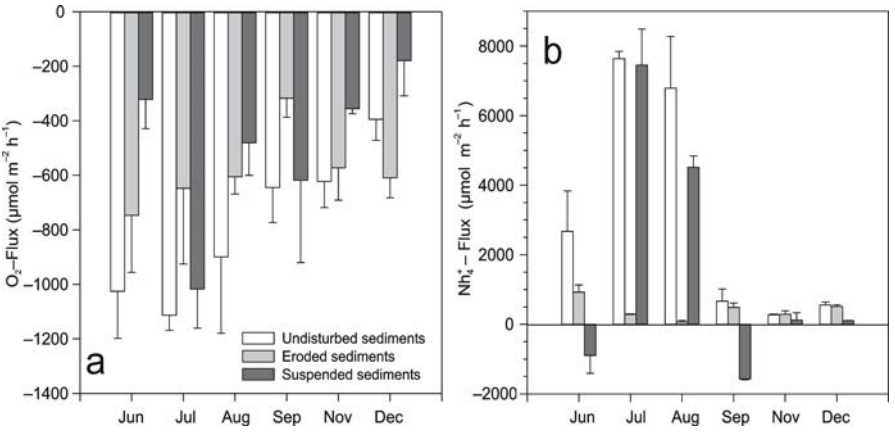

Fig. 3.25. Measurements of oxygen consumption and ammonia fluxes (dark incubation) of undisturbed, eroded, and suspended sediments sampled from the station Z during the period from June to December 2004. The *bars* represent mean values ±SD ($n = 3$)

sediments by their biogenic structures (burrows, tubes). Sediments of the groyne field were colonized by the oligochaetes *Tubifex tubifex* which live in tubes coated with mucilagenous material. A significant direct correlation was found between the biomass of the worms and the contents of EPS (Fig. 3.24b). This especially applies to the sandy mud sediments at the edges of the groyne field which were characterized by high worm biomass, high contents of EPS, and low ratios of organic carbon to nitrogen, characteristic for EPS.

EPS are especially known for their high adsorption capacity for metals (Schlekat et al. 1998). With increasing erosion of particles and EPS, the release of metals from the sediments increased (Fengler et al. 2006). The comparable patterns of mobilization of cadmium, lead, mercury, zinc, and copper pointed to the unspecific binding of the metals to EPS.

Erosion of sediments caused a stimulation of the activities of microorganisms associated with the resuspended particles. Measurements of the respiration revealed that the sum of the oxygen consumption of the eroded and the resuspended sediments clearly exceeded the oxygen consumption of the undisturbed sediments (Fig. 3.25a). In summer microbial activities associated with resuspended sediments caused a considerable release of ammonia (Fig. 3.25b). Oxygen consumption and liberation of ammonia represent major processes causing the eutrophication of aquatic environments.

3.5.5 Conclusions

The stability of the sediments of the river Elbe was reflected in sediment-specific erosion curves that varied seasonally and spatially due to variations in the chemical properties and microbial colonization of the eroded sediment particles. Exposed sandy mud sediments at the edges of the groyne field showed higher critical shear stress as compared to the more muddy sediments in the center. With increasing stability, fewer particles of larger size were liberated. Based on correlations between critical shear stress

and content of EPS of the particles released it is suggested that deposited planktonic microalgae and oligochaetes contributed to the EPS content and act as biostabilizers in the sediments in the groyne field.

The fine sediment particles were main contributors to the nutrient and pollution load in the water column. Fractionation of particles according to their sedimentation speed showed that the fine fraction was characterized by enhanced contents of carbon, nitrogen and phosphorus as well as enhanced microbial colonization and activity. Particularly during the summer, bacteria associated with resuspended fine particles contributed to the eutrophication of water by high consumption of oxygen and liberation of ammonia.

Based on our observations we conclude that the sediment stability is a key parameter that predicts the erosion risk of riverine sediments. Sediments with a low stability (low critical shear stress) act as sources of nutrients and pollutants, whereas sediments with a high stability (high critical shear stress) function as sinks which have a high potential to bind nutrients and pollutants. To minimize the erosion risk of fine-grained cohesive sediments in riverine environments enhanced knowledge on the impact of sediment properties and (micro)benthic colonization on sediment stability is required for a successful application of sediment management strategies.

Acknowledgments

This study was part of the interdisciplinary research project "Sedimentdynamik und Schadstoffmobilität in Fließgewässern" (sediment dynamics and pollutant mobility in rivers (SEDYMO)) supported by the German Federal Ministry of Education and Research (BMBF). The authors are grateful to Lars Kreuzer and Ingrid Kreuzer for technical assistance. The port authority, Hamburg, and the Wasser- und Schifffahrtsamt, Lauenburg, is thanked for the help during sampling.

References

de Brouwer JFC, Bjelic S, de Deckere EMGT, Stal LJ (2000) Interplay between biology and sedimentology in a mudflat (Biezelingse Ham, Westerschelde, The Netherlands). Continental Shelf Res 20:1159–1177

de Brouwer JFC, Stal LJ (2001) Short-term dynamics in microphytobenthos distribution and associated extracellular carbohydrates in surface sediments of an intertidal mudflat. Mar Ecol Prog Ser 218:33–44

de Brouwer JFC, Wolfstein K, Ruddy GK, Jones TER, Stal LJ (2005) Biogenic stabilization of intertidal sediments: the importance of extracellular polymeric substances produced by benthic diatoms. Microb Ecol 49:501–512

Decho AW (1990) Microbial exopolymer secretion in ocean environments: their role(s) in webs and marine processes. Oceanography and Marine Biology: An Annual Review 28:73–153

Decho AW, Kawaguchi T, Allison MA, Louchard EM, Reid RP, Stephens FC, Voss KJ, Wheatcroft RA, Taylor BB (2003) Sediment properties influencing upwelling spectral reflectance signatures: The "biofilm gel effect". Limnol Oceanogr 48:431–443

Fengler G, Köster M, Meyer-Reil LA (2006) Mikrobielle Stoffumsätze an resuspendierten Sedimenten. Final report of the interdisciplinary BMBF-project: Sediment Dynamics and Pollutant Mobility in Rivers (SEDYMO)

Findlay RH, King GM, Watling L (1989) Efficiacy of phospholipids analysis in determining microbial biomass in sediments. Appl Environ Microbiol 55:2888–2893

Flemming HC, Wingender J (2001) Relevance of microbial extracellular polymeric substances (EPSs). Part II: Technical aspects. Wat Sci Technol 43:9–16

Graf G, Rosenberg R (1997) Bioresuspension and biodeposition: A review. J Mar Systems 11:269–278

Grant J, Gust G (1987) Prediction of coastal sediment stability from photopigment content of mats of purple bacteria. Nature 330:244–246

HELCOM, Helsinki Commision (1988) Guidelines for the Baltic monitoring programme for the third stage. Baltic Sea Environ Proc 27D: biological determinants. Helsinki Commission, Helsinki, pp 1–60

Köster M, Dahlke S, Meyer-Reil LA (1997) Microbiological studies along a gradient of eutrophication in a shallow coastal inlet in the southern Baltic Sea (Nordrügensche Bodden). Mar Ecol Prog Ser 152:27–39

Köster M, Meyer-Reil LA (2002) Ecology of marine microbial biofilms. In: Bitton G (ed) The encyclopedia of environmental microbiology. John Wiley & Sons, Inc., New York, pp 1081–1091

Meyercordt J, Meyer-Reil LA (1999) Primary production of benthic microalgae in two shallow coastal lagoons of different trophic status in the southern Baltic Sea. Mar Ecol Prog Ser 178:179–191

Meyer-Reil LA (1983) Benthic response to sedimentation events during autumn to spring at a shallow-water station in the western Kiel Bight. II. Analysis of benthic bacterial populations. Mar Biol 77:247–256

Meyer-Reil LA (2006) Mikrobiologie des Meeres. Eine Einführung. Facultas UTB, Stuttgart

Nichols CM, Ladiére SG, Bowman JP, Nichols PD, Gibson JAE, Guézennec J (2005) Chemical characterization of exopolysaccharides from Antarctic marine bacteria. Microb Ecol 49:578–589

Paterson DM, Tolhurst TJ, Black KS, Shayler SA, Mather S, Black I (1999) Measuring the in situ erosion shear stress of intertidal sediments with the cohesive strength meter (CSM). Est Coast Shelf Sci 49:281–294

Petersen W, Hong J, Williamoski C, Wallmann K (1996) Release of trace contaminants during reoxidation of anoxic sediment slurries in oxic water. Arch Hydrobiol Spec Issues Advanc Limnol 47:295–305

Ploug H, Zimmermann-Timm H, Schweitzer B (2002) Microbial communities and respiration on aggregates in the Elbe Estuary, Germany. Aquat Microb Ecol 27:241–248

Rieling T (2000) Remineralisation organischen Materials in Boddengewässern Mecklenburg-Vorpommerns unter besonderer Berücksichtigung der Bedeutung von Partikeln und Aggregaten. Ph.D. thesis, University Greifswald

Roast SD, Widdows J, Pope N, Jones MB (2004) Sediment-biota interactions: mysid feeding activity enhances water turbidity and sediment erodability. Mar Ecol Prog Ser 281:145–154

Schlekat CE, Decho AW, Chandler GT (1998) Sorption of cadmium to bacterial extracellular polymeric sediment coatings under estuarine conditions. Environ Toxicol Chem 17:1867–1874

Shanks AL, Edmondson EW (1989) Laboratory-made artificial marine snow: A biological model of the real thing. Mar Biol 101:463–470

Shimeta J, Amos CL, Beaulieu SE, Katz SL (2004) Resuspension of benthic protists at subtidal coastal sites with differing sediment composition. Mar Ecol Prog Ser 259:103–115

Sutherland TF, Amos CL, Grant J (1998) The effect of buoyant biofilms on the erodibility of sublittoral sediments of a temperate microtidal estuary. Limnol Oceanogr 43:225–235

Tsai CH, Lick W (1986) A portable device for measuring sediment resuspension. J Great Lakes Res 12:314–321

Westrich B, Förstner U (2005) Sediment dynamics and pollutant mobility in rivers (SEDYMO) assessing catchment-wide emission-immission relationships from sediment studies. BMBF coordinated research project SEDYMO (2002–2006). J Soils Sediments 5:197–200

Widdows J, Brinsley MD, Bowley N, Barrett C (1998) A benthic annular flume for in situ measurement of suspension feeding/deposition rates and erosion potential of intertidal cohesive sediments. Est Coast Shelf Sci 46:27–38

Widdows J, Brinsley MD, Salkeld PN, Lucas CH (2000) Influence of biota on spatial and temporal variation in sediment erodability and material flux on a tidal flat (Westerschelde, The Netherlands). Mar Ecol Prog Ser 194:23–37

Widdows J, Brinsley MD, Pope ND, Staff FJ, Bolam SG, Somerfield PJ (2006) Changes in biota and sediment erodability following the placement of fine dredged material on upper intertidal shores of estuaries. Mar Ecol Prog Ser 319:27–41

Ziervogel K (2003) Aggregation and transport behaviour of sediment surface particles in Mecklenburg Bight, south-western Baltic Sea, affected by biogenic stickiness. Ph.D. thesis, University Rostock.